

https://doi.org/10.3799/dqkx.2023.079



(U-Th)/He 定年及影响因素研究进展

杨莉^{1,2,3}, 杨静^{1,2*}, 田鹏⁴, 施炜^{1,2}, 李肖⁵

1. 中国地质科学院地质力学研究所, 北京 100081
2. 自然资源部活动构造与地质安全重点实验室, 北京 100081
3. 中国地质大学科学研究院, 北京 100083
4. 云南省地震局, 云南昆明 650224
5. 山东黄金地质矿产勘查有限公司, 山东烟台 261400

摘要: (U-Th)/He 同位素定年以其低温敏感性 (70 °C) 为造山带隆升-剥蚀速率的时空格架构建、油气成藏时间约束、沉积盆地埋藏历史恢复、矿床剥蚀保存研究及古地形地貌重塑等提供了精确的时间-温度演变模型, 应用前景广阔。理解矿物封闭温度、内部结构、⁴He 扩散机制、铀-钍分带效应等是 (U-Th)/He 数据解释的核心所在。本文详尽论述了 (U-Th)/He 技术研究, 包括测年适宜对象及在不同地质领域的应用、测试方法的发展及标准矿物结果, 着重归纳了造成年龄偏差的因素, 并简述了主要矿物的辐射损伤机制。研究表明, 我国 (U-Th)/He 定年技术从非稀释剂法测定发展至单颗粒激光熔融技术, 再延续到准分子激光剥蚀系统 RESolution 下的原位微区双定年技术, FCT 锆石、Durango 磷灰石及蓬莱锆石的测定结果与国际标定年龄在误差范围内一致, 并自主开发了 MK-1 磷灰石标样, 目前该技术已相对成熟, 能有效保存 ⁴He 的多数铀-钍副矿物均可成为适宜定年对象, 本文总结了有效规避矿物包裹体、矿物粒径、 α 粒子射出及植入效应、成分环带等影响因素的策略, 可为国内学者在 (U-Th)/He 数据解释中提供帮助和参考。

关键词: (U-Th)/He; 影响因素; 磷灰石; 锆石; 地球化学; 同位素。

中图分类号: P597

文章编号: 1000-2383(2024)09-3155-27

收稿日期: 2023-02-28

The Research Advances of (U-Th)/He Dating and Influencing Factors

Yang Li^{1,2,3}, Yang Jing^{1,2*}, Tian Peng⁴, Shi Wei^{1,2}, Li Xiao⁵

1. Institute of Geomechanics, Chinese Academy of Geological Sciences, Beijing 100081, China
2. Key Laboratory of Active Tectonics and Geological Safety, Ministry of Natural Resources, Beijing 100081, China
3. Institute of Earth Sciences, China University of Geosciences, Beijing 100083, China
4. Yunnan Earthquake Agency, Kunming 650224, China
5. Shandong Gold Geology and Mineral Exploration Co., Ltd., Yantai 261400, China

Abstract: (U-Th)/He isotopic dating with its low-temperature sensitivity (70 °C), provides an accurate time-temperature evolution model for the construction of temporal-spatial framework of uplift and denudation rates in orogenic belts, temporal constraints on hydrocarbon formation, recovery of burial history in sedimentary basins, the study of denudation and preservation of mineral deposits, and reconstruction of paleotopography and geomorphology, with promising applications. Understanding mineral closure

基金项目: 国家自然科学基金项目 (Nos. 41873063, 92062217, 42241161); 中国地质调查局地质调查项目 (No. DD20221644); 2021 年度中国地质大学 (北京) 研究生创新资助项目 (No. YB2021YC021)。

作者简介: 杨莉 (1987-), 女, 博士, 主要从事低温热年代学方法及应用研究。ORCID: 0000-0001-5168-3591. E-mail: Yangli0211luck@126.com

* **通讯作者:** 杨静, ORCID: 0000-0002-7828-1055. E-mail: yangjing_822822@163.com

引用格式: 杨莉, 杨静, 田鹏, 施炜, 李肖, 2024. (U-Th)/He 定年及影响因素研究进展. 地球科学, 49(9): 3155-3181.

Citation: Yang Li, Yang Jing, Tian Peng, Shi Wei, Li Xiao, 2024. The Research Advances of (U-Th)/He Dating and Influencing Factors. *Earth Science*, 49(9): 3155-3181.

temperatures, internal structure, ^4He diffusion mechanisms, and uranium-thorium zoning effects are keys to interpreting (U-Th)/He data. A detailed discussion of (U-Th)/He technical studies is presented, including the appropriate target minerals and different geological applications for dating, the development of test methods and standard references, a focus on the factors that contribute to age bias, and a brief description of the radiation damage mechanisms for the major minerals. Research has shown that China's (U-Th)/He dating technology has advanced significantly, progressing from the non-dilution method to the single-particle laser fusion technique, and subsequently to the in-situ micro-area dual dating method using the RESOLUTION excimer laser ablation system. Measurement results from FCT zircon, Durango apatite, and Penglai zircon align closely with international calibration ages, falling within the expected margin of error. Moreover, an MK-1 apatite standard sample has been developed independently, indicating the maturity of the technology. Most of the uranium-thorium bearing minerals that have effectively preserved ^4He can be suitable objects for dating. A summary of strategies to effectively avoid the effects of mineral inclusions, mineral grain size, α -particle ejection and implantation effects, and compositional ring-banding can help Chinese scholars interpret (U-Th)/He data.

Key words: (U-Th)/He; influencing factors; apatite; zircon; geochemistry; isotopes.

0 引言

稀有气体元素(或称惰性气体,包括氦(He)、氖(Ne)、氩(Ar)、氪(Kr)、氙(Xe)、氡(Rn)六个元素),以化学性质稳定、地球中含量稀少为特征.其中,氦半衰期极短(3.82 d)(Porcelli and Turekian, 2003),氦和氡无论在太阳系中还是地球上其丰度都极稀少,难以准确测定,均未能在地球科学研究中发挥作用.近年来随着质谱测试精度的提高,稀有气体研究进入鼎盛时期.例如,利用地下水中Ne、Ar、Kr、Xe的浓度可获取古气候演变相关信息(Peeters *et al.*, 2003),洋壳中He、Ne同位素可用于地幔中惰性气体再循环的研究(Moreira *et al.*, 2003).其中 ^4He 具有年代积累效应被用于(U-Th-Sm)/He、 $^4\text{He}/^3\text{He}$ 及(U-Th)/Ne同位素定年研究.相较之下,(U-Th)/He方法对低温热事件的高度敏感性(可低至70 °C),促成其在典型造山带、热液矿床、沉积盆地隆升-剥露速率厘定中被广泛应用(McInnes *et al.*, 2005; Wang *et al.*, 2016; 袁万明, 2016; 郑德文等, 2016; 冯乾乾等, 2018; 杨莉等, 2018, 2021; Pang *et al.*, 2019; Li *et al.*, 2021; 郭超等, 2022; 林旭等, 2022; 吴立群等, 2022).近年来,该方法在限定火山喷发时代(Schmitt *et al.*, 2013)、约束河流下切速率(Adams *et al.*, 2009; Liu *et al.*, 2018)、厘定活动构造时限(Tian *et al.*, 2012; Tao *et al.*, 2019; Yu *et al.*, 2019; Wang *et al.*, 2022)等地质事件格架构建中优势显著,甚至可在古老天体行星冲击事件的研究中发挥作用(Min *et al.*, 2003, 2004),彰显出有别于其他放射性同位素定年技术难以替代的应用前景.就目前发表的成果来看,(U-Th)/He年龄跨度很大,从几千年(锆石(U-Th)/He 14~12 ka;

Schmitt *et al.*, 2014)到4.55 Ga(Acapulco 陨石),为认识地球浅表地质过程提供了新的途径.技术上, ^4He 扩散机制研究日趋成熟,从原子上升到晶胞尺度研究(Djimbi *et al.*, 2015),利用拉曼光谱、透射电子显微镜和原子微探针技术,可以精准识别矿物的辐射损伤积累-退火机制,为数据的合理解释奠定了基础.连续升温加热方式(Idleman *et al.*, 2018; McDannell *et al.*, 2018a)可有效识别磷灰石中 ^4He 异常扩散,对 ^4He 释气造成的数据分散提供参考依据;纳米微结构层次的观察结合氧化物热年代学分析(Moser *et al.*, 2017)可以实现对深部热液系统、断层形成时代和矿床保存的直接定年.然而,对年龄结果的正确判读一直是制约(U-Th)/He推广的重要因素,对定年原理、扩散机制及测试方法的准确理解,更有助于提供合理的解释.该方法的应用是基于衰变体系中所有子体同位素处于长期平衡状态以及矿物晶体不存在原始 ^4He 的前提.此假设限于理想状态,即大气氦浓度极低($\sim 5 \times 10^{-6}$),多数矿物中不会存在大气来源的 ^4He .对于富稀土、贫U、Th的磷酸盐矿物,上述假设只在约350 ka的结晶期内成立.在年轻火山岩中,不得不考虑放射性衰变稳态平衡的影响,尤其是结晶年龄小于1 Ma的样品,需采取 ^{238}U 系非平衡年龄方程进行校正(Farley, 2002; Zheng *et al.*, 2006).年龄计算中需考虑 ^{147}Sm 含量,如在大多数矿物中 ^{147}Sm 对 ^4He 的贡献通常小于U和Th(不到总 ^4He 积累量的1%),可忽略不计.但磁铁矿和石榴石中, ^{147}Sm 浓度可观($1 \times 10^{-6} \sim 3 \times 10^{-6}$)(Blackburn *et al.*, 2008),此时 ^{147}Sm 对 ^4He 的贡献须考虑在内.矿物粒径、颗粒完整程度以及包裹体的影响会造成年龄值的偏差. α 粒子的射出和植入效应、成分环带和辐射损伤效

应等因素亦会对年龄准确度产生影响。基于此,本文拟分析目前不同矿物进行(U-Th)/He测试的适宜性,探讨该技术分析的研究进展,归纳目前研究中提及的对(U-Th)/He年龄结果的干扰因素,以期有效提高定年的成功率,为大地地质研究者提供借鉴和参考。

1 (U-Th)/He测年矿物

理论上,富含铀的矿物均可用于(U-Th)/He测年,实际上,在地表甚至上地壳热流条件下仍能有效保存 ^4He 的矿物更适宜于定年。扩散机制的深入研究和测试技术的完善,使磷灰石和锆石更易获得理想的定年结果,榍石次之。这些矿物是目前(U-Th)/He定年中最广泛使用的矿物(Yu *et al.*, 2020)。独居石中Th和U含量(质量分数)分别高达15%、2%,晶体内 ^4He 积累快速。其晶体结构比磷灰石致密, ^4He 扩散速率低,适用于(U-Th)/He定年(Parrish, 1990)。不过,其封闭温度对于化学成分依赖性很强(Boyce and Hodges, 2005),相对富集轻稀土元素的独居石 ^4He 扩散速度更快(Cherniak and Watson, 2011)。Th含量较高的独居石由于晶格的成对取代效应会减缓 ^4He 扩散速度(Peterman *et al.*, 2014),导致即便同一样品不同颗粒得到的封闭温度值变化较大(如206~286 °C; Boyce and Hodges, 2005)。对其冷却年龄的解释不得不考虑复杂化学分带的影响(Flowers *et al.*, 2023a)。磷钇矿内放射性核素浓度远高于磷灰石、榍石及锆石, ^4He 的快速积累为活跃构造带内相对年轻的冷却事件提供了精细厘定的可能性。然而,磷钇矿难以获取且晶体尺寸普遍较小,致使其应用受限(Anderson *et al.*, 2019)。金红石是蓝片岩、榴辉岩和麻粒岩等高温高压变质岩以及某些深成岩中的典型含铀副矿物,其封闭温度接近锆石,可为区域性火成岩和变质作用演化研究提供重要参考,尤其是金红石碎屑热年代学可为沉积物物源分析、源岩年龄重建和源区构造隆起时限约束提供关键证据(Robinson *et al.*, 2019)。石榴石因离子孔隙率极低,使其成为硅酸盐矿物中最具 ^4He 保存性的矿物,其封闭温度约590~630 °C,可用于示踪大陆地壳流体和测年(Dunai and Roselieb, 1996),石榴石斑晶(U-Th)/He定年为年轻火山岩喷发时限的厘定提供了除K-Ar、 $^{40}\text{Ar}/^{39}\text{Ar}$ 和 ^{14}C 等方法以外的有力补充(Aciego *et al.*, 2003)。萤石铀含量高达100 $\mu\text{g}/\text{g}$ (Pi

et al., 2005),可直接用于测定萤石矿床年代,以弥补萤石裂变径迹与晶体缺陷以及微小流体包裹体难以有效区分的缺陷,突破了萤石Sm-Nd方法等时线年龄精度不高、Sm/Nd初始同位素比值存在非均质性的限制(Groënlie *et al.*, 1990; Jellinek and Kerr, 1999)。虽然橄榄石中U和Th浓度较低,但其仍被成功应用于第四纪玄武岩年代测定中,其多重来源 ^4He 的辨析是获取有效地质年龄的关键所在(Aciego *et al.*, 2010)。赤铁矿、针铁矿及磁铁矿等铁氧化物的(U-Th)/He年龄可用于金属矿床(Fanale and Kulp, 1962)、镁铁质火山岩(Blackburn *et al.*, 2007)、超镁铁质和镁铁质岩石等变质作用(Cooperdock and Stockli, 2016; Schwartz *et al.*, 2020)、河谷沉积型铁矿(Vasconcelos *et al.*, 2013)时代限定、风化速率估算(Heim *et al.*, 2006; Monteiro *et al.*, 2014)等,具有广阔应用前景。Ault *et al.*(2015)尝试运用断层带中赤铁矿(U-Th)/He数据提供 $10^5\sim 10^6$ a时间尺度上,与断层滑移相关的岩石热异常的可能性,为直接测定断层滑动时代(Calzolari *et al.*, 2018)和解释地震活动(Calzolari *et al.*, 2020)提供了新思路。然而,完全释放铁氧化物中的 ^4He 通常需较高温度。例如,赤铁矿完全释放 ^4He 温度需高于1 000 °C,而加热至950 °C会触发赤铁矿铀丢失效应,导致年龄偏高。因此对铀丢失效应的量化是未来赤铁矿(U-Th)/He年代学中亟待解决的问题(Hofmann *et al.*, 2020)。在地表环境下,方解石及霏石等碳酸盐矿物晶格中亦可有效保存 ^4He 。因此,断层裂隙中充填的方解石He年龄可提供成矿及断层流体运移的关键信息(Cros *et al.*, 2014; Powell *et al.*, 2018)。不过,由于受富含包裹体及多重扩散域的影响,获取理想结果并非易事。在实际定年中,优先选择直径 >2 mm的方解石碎片(等效于铀浓度 $>0.3\times 10^{-6}$)或许可以奏效(Copeland *et al.*, 2007)。寒武纪-三叠纪地层中普遍存在的磷酸盐微体化石(如牙形石)的主要成分是羟基磷灰石,牙形石(U-Th)/He年代学可填补海相碳酸盐岩及页岩热年代学数据研究中的空白。值得注意的是,其铀(U)、钍(Th)、稀土元素(REE)平均浓度及微观结构均会对年龄结果产生影响(Tyrrell *et al.*, 2016)。Jourdan and Eroglu (2017)利用 ^4He 和放射成因氩($^{40}\text{Ar}^*$)在陨石从其宿主行星到地球的过程中会遭受不同程度损失的特性,成功判定了水星、金星中的陨石,将其应用研究扩展到了天体研究领域。

表 1 不同矿物(U-Th)/He 封闭温度总结
Table 1 Compilation of different minerals (U-Th)/He closure temperatures

矿物	封闭温度(°C)	参考文献
磷灰石	75(冷却速率为 10 °C/Ma)	Wolf <i>et al.</i> , 1996
	80~90	Crowley <i>et al.</i> , 2002
	88±5	Chang <i>et al.</i> , 2012
	72	van Soest <i>et al.</i> , 2011
	62(粒径 60 μm)	Flowers <i>et al.</i> , 2009
氯磷灰石	69	Farley, 2000
	18(冷却速率 0.3°C/Ma)	Min <i>et al.</i> , 2013
锆石	175~195(冷却速率 10 °C/Ma)	Reiners <i>et al.</i> , 2002; Tagami <i>et al.</i> , 2003
	>200	蔡长娥等, 2020b
	144~216(冷却速率为 10°C/Ma)	喻顺等, 2019
独居石	206±24, 230±4, 286±13	Boyce and Hodges, 2005
	224	Farley and Stockli, 2002
	262~291	Peterman <i>et al.</i> , 2014
磷钇矿	35~75	Anderson <i>et al.</i> , 2019
	115	Farley and Stockli, 2002
	190	Farley, 2007
榍石	220~190	Reiners and Farley, 1999
	100~180	Stockli and Farley, 2004
金红石	220~235	Stockli <i>et al.</i> , 2007
	180~200	Crowhurst <i>et al.</i> , 2002
	155~159	Robinson <i>et al.</i> , 2019
石榴石	200~300	Seman <i>et al.</i> , 2014
	590~630	Dunai and Roselieb, 1996
萤石	60±5	Evans <i>et al.</i> , 2005
	200	Pi <i>et al.</i> , 2005
	169~46	Wolff <i>et al.</i> , 2016
磁铁矿	~250±50	Blackburn <i>et al.</i> , 2007
赤铁矿	140~240	Evenson <i>et al.</i> , 2014
	178~218	Lippolt <i>et al.</i> , 1993
方解石	60~80	Copeland <i>et al.</i> , 2007
牙形石	60~70(冷却速率为 10 °C/Ma)	Peppe and Reiners, 2007
	50~90	Bidgoli <i>et al.</i> , 2018
	60~67	蔡长娥等, 2020a
陨磷钙钠石	94~112(冷却速率为 0.3~2.6 °C/Ma)	Min <i>et al.</i> , 2013
尖晶石	200~300	Cooperdock and Stockli, 2018
斜锆石	450~500	Metcalf and Flowers, 2013
钙钛矿	>300	Stanley and Flowers, 2016
橄榄石	697	Hart, 1984
	648	Trull and Kurz, 1993
单斜辉石	456	Trull and Kurz, 1993
白云母	41	
透长石	52	
角闪石	79~106	
普通辉石	94	Lippolt and Weigel, 1988
霞石	152	
无水钾镁矾	87	
绿帘石	63	Niculescu and Reiners, 2005

综上,不同来源的多种副矿物均可以作为(U-Th)/He定年的适宜对象,其有效封闭温度的差异使其可以限定不同温度的热事件.表1汇总了目前已发表的(U-Th)/He体系中不同矿物的封闭温度.

2 (U-Th)/He方法分析进展

近年来,国内外相继建立(U-Th)/He实验室,各个实验室测试流程存在差异.发展初期,人们采取真空电阻炉加热法加热提取 ^4He ,继而采用X射线荧光光谱法(X-ray fluorescence,简称XRF)或热电质谱法(thermal ionization mass spectrometry,简称TIMS)进行U、Th含量分析.然而,该方法耗时长、系统误差大,且易出现温度过冲效应,不利于 ^4He 扩散研究(Zeitler *et al.*, 1987).此后,科学家们开始尝试采用Nd-YAG(Neodymium-doped Yttrium Aluminium garnet)或 CO_2 激光器加热封存单颗粒矿物的箔(铌)管(厚0.025 mm,纯度达99.99%)提取 ^4He ,再利用等离子质谱(inductively coupled plasma mass spectrometer,简称ICP-MS)同位素稀释法完成U、Th含量测试,属目前使用最广泛的技术(杨静等,2014;Wang *et al.*, 2020; Zhang *et al.*, 2020; Yu *et al.*, 2022).尽管激光加热方法的 ^4He 本底值远低于真空炉方法,具备明显优越性,但此种方式假设U、Th均匀分布,实际中矿物很难达到此标准.激光原位微区技术则能避免上述缺陷,即无需进行 α 粒子射出效应的校正,能够实现对子、母体同位素分布不均匀样品的测试.利用准分

子激光器、紫外线激光和二极管激光等对抛光矿物表面凹区进行烧蚀,通过精确测定剥蚀坑体积来获取 ^4He 、U、Th和Pb含量.这种方法具有精度高、效率高、免校正,可同时获取U-Pb、(U-Th)/He年龄和微量元素含量诸多优势,但对矿物粒径以及U、Th等母体同位素含量要求较高(粒径 $>100\ \mu\text{m}$,U、Th含量 $>1\ \mu\text{g/g}$),并不适用于年轻样品($<1\ \text{Ma}$).因此,目前该方法仅在独居石(Boyce *et al.*, 2006)、磷灰石(van Soest *et al.*, 2008)及锆石(Tripathy-Lang *et al.*, 2013)等少数富U-Th矿物中取得理想结果.激光剥蚀中侧向加热效应会增加 ^4He 含量,使得 ^4He 测量值偏大.不规则形态剥蚀坑体积的精确测定复杂,不同矿物激光剥蚀速率的差异性及缺少标准样品进行比对等都是制约原位激光微区(U-Th)/He技术发展的因素(Foeken *et al.*, 2006).

前已述及,目前国内外(U-Th)/He测试主流方法为传统激光熔融技术,对标准物质有较大依赖性.目前主要开发的标准物质为磷灰石和锆石,其他矿物的标准物质尚在研制中,当前(U-Th)/He方法使用的标样分述如下:

(1)蓬莱锆石:蓬莱锆石是2010年中国科学院地质与地球物理研究所开发的U-Pb定年、O、Hf同位素分析的固体标样.其产于海南岛北部碱性玄武岩中,具有较高的U含量和Th/U比值(Li *et al.*, 2010),蓬莱锆石的U-Pb同位素年龄如表2所示,不同学者获得的蓬莱锆石(U-Th)/He年龄和U-Pb年龄结果一致(Li *et al.*, 2017; Yu *et al.*, 2020)(图1a),表明经历快速冷却的蓬莱锆石具备锆石(U-Th)/He标准参考物质的潜力.

表2 蓬莱锆石同位素年龄统计

Table 2 Isotopic age of Penglai zircon reference materials

年龄(Ma)	研究方法	资料来源
4.393 \pm 0.041	TIMS U-Pb	Li <i>et al.</i> , 2010
4.36 \pm 0.12	SIMS U-Pb	
4.2 \pm 0.12		Chew <i>et al.</i> , 2014
4.3 \pm 0.2		Crowley <i>et al.</i> , 2014
4.1 \pm 0.2	LA-ICP-MS U-Pb	Yu <i>et al.</i> , 2010
4.2 \pm 0.12		Petrus and Kamber, 2012
PL1: 4.29 \pm 0.03		
PL2: 3.95 \pm 0.05	LA-MC-ICP-MS U-Pb	
		Yu <i>et al.</i> , 2020
PL1: 4.12 \pm 0.10		
PL2: 3.07 \pm 0.25	(U-Th)/He	
4.06 \pm 0.35		Li <i>et al.</i> , 2017

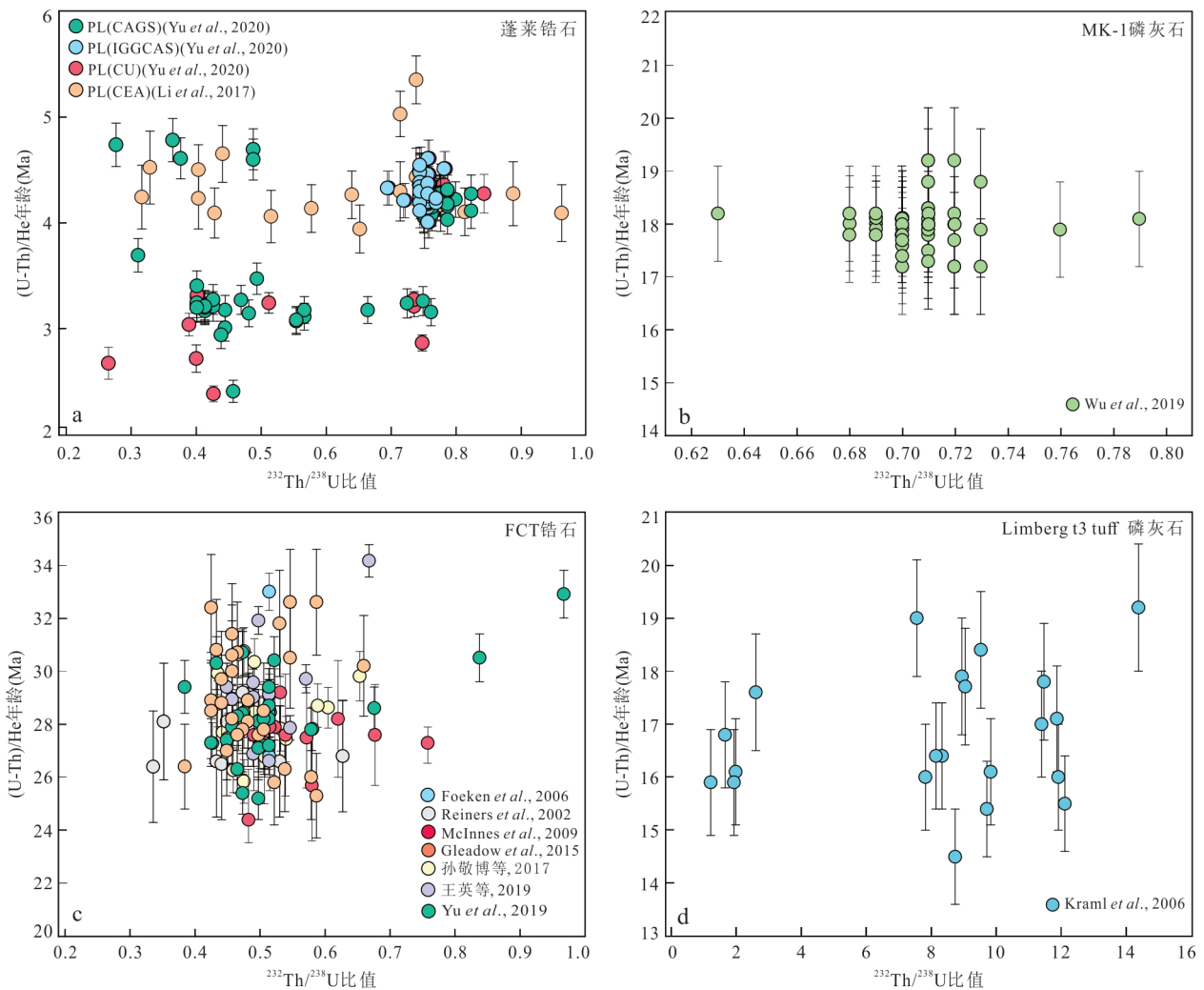


图1 蓬莱锆石(a)、MK-1磷灰石(b)、FCT 锆石(c)及Limberg t3 凝灰岩(d)(U-Th)/He年龄与 $^{232}\text{Th}/^{238}\text{U}$ 比值的关系

Fig.1 (U-Th)/He age versus $^{232}\text{Th}/^{238}\text{U}$ ratio of PengLai zircons (a), MK-1 apatite (b), FCT zircons (c) and Limberg t3 tuff (d) CAGS. Chinese Academy of Geological Sciences; CEA. China Earthquake Administration; IGGCAS. Institute of Geology and Geophysics, Chinese Academy of Sciences; CU. Curtin University

(2) MK-1 磷灰石: 采自缅甸 Mogok 地区的 MK-1 磷灰石是 2019 年中国科学院地质与地球物理研究所新开发的磷灰石标准物质. 其属于极高透明度的蓝色厘米级巨晶宝石, 30 个磷灰石碎片分别采用原位方法和传统方法进行 (U-Th)/He 年代测定, 年龄为 (18.0 ± 0.2) Ma, 且结果复现性极好 (图 1b) (Wu *et al.*, 2019).

(3) FCT (Fish Canyon Tuff) 锆石: 这是目前使用最多的标准物质, 产于美国科罗拉多州圣胡安山脉的渐新世火山灰层中, 其核幔边界、环带结构复杂, 是典型的 FCT 锆石 (长度 $< 250 \mu\text{m}$, 宽度 $< 150 \mu\text{m}$), 可见明显铀、钍分带. 最近的 FCT 锆石 (U-Th)/He 定年结果陆续发表, 如 (28.3 ± 0.4) Ma (Gleadow *et al.*, 2015)、 $(28.8 \pm$

$3.1)$ Ma (王英等, 2019)、 (28.38 ± 0.34) Ma (喻顺等, 2019)、 (28.18 ± 0.51) Ma (孙敬博等, 2017), 其年龄区间介于 27.2~28.8 Ma (图 1c), 与 $^{40}\text{Ar}/^{39}\text{Ar}$ 、U-Pb 等方法年龄结果基本一致.

(4) Limberg t3 凝灰岩: 该样品来自德国莱茵河上游地堑中新世沉积岩序列中的 Limberg 火山岩, 其高钾富铀, 为 $^{40}\text{Ar}/^{39}\text{Ar}$ 、FT (Fission Track)、(U-Th)/He 多个年代学体系的标准矿物. 其磷灰石 FT 年龄为 $16.8 (-1.2, +1.3)$ Ma, 榧石 (U-Th)/He 年龄为 (16.5 ± 1.0) Ma, 磷灰石 (U-Th)/He 年龄为 (16.7 ± 1.0) Ma, 透长石 $^{40}\text{Ar}/^{39}\text{Ar}$ 年龄为 (16.3 ± 0.4) Ma (图 1d). 其中透长石、磷灰石及榧石矿物粒径较大, 榧石和磷灰石亦达 0.3~0.5 mm, 也是进行 (U-Th)/

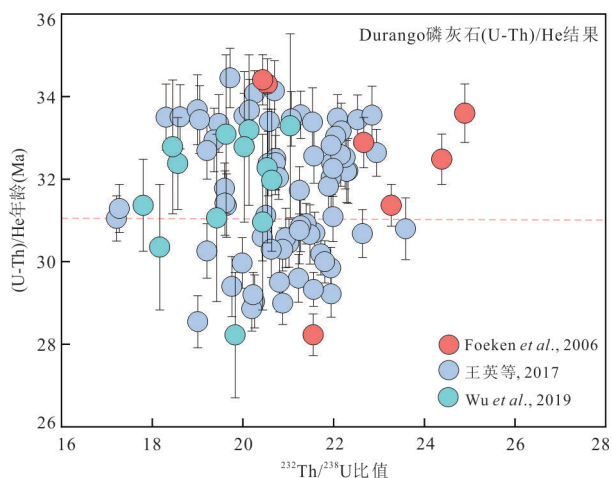


图2 Durango 磷灰石 (U-Th)/He 年龄与 $^{232}\text{Th}/^{238}\text{U}$ 比值的
关系

Fig.2 (U-Th)/He age versus $^{232}\text{Th}/^{238}\text{U}$ ratio of Durango
apatite

He 定年的理想标准矿物 (Kraml *et al.*, 2006)。

(5) Durango 磷灰石: Durango 磷灰石是研究程度较高的宝石级标准物质, 其 K-Ar 年龄为 (30.3 ± 0.4) Ma 和 (30.9 ± 0.4) Ma (Naeser and Fleischer, 1975)。单晶体的 U、Th 分布均匀, 透明度高, 几乎不含包裹体, 且易获得较大粒径的单颗粒。因此, 无需进行 α 粒子射出效应校正, 其 $^{40}\text{Ar}/^{39}\text{Ar}$ 年龄为 (31.44 ± 0.18) Ma (McDowell *et al.*, 2005), (U-Th)/He 年龄为 (31.02 ± 1.01) Ma、 (32.1 ± 1.7) Ma (House *et al.*, 2000)、 (31.7 ± 1.1) Ma (Wu *et al.*, 2019)、 (31.71 ± 1.55) Ma (王英等, 2017)、 (32.8 ± 1.8) Ma (Foeken *et al.*, 2006)。Durango 磷灰石 (U-Th)/He 年龄介于 31~33 Ma (图 2)。

此外, Tian *et al.* (2017) 提出的斯里兰卡 LGC-1 天然锆石 ((476.4 ± 5.7) Ma) 也成为了未来 (U-Th)/He 测试中有潜力的标准物质。

3 (U-Th)/He 年龄影响因素

3.1 矿物包裹体

高 U、Th 矿物包裹体会产生过剩 ^4He , 导致年龄异常偏大, 在热液磷酸盐矿物中尤甚。Lippolt *et al.* (1994) 指出, 由于热液磷灰石封闭温度极低, 加之存在过剩 ^4He , 极易导致年龄结果偏老。相比于热液磷灰石, 深成岩中的磷灰石可能更适合 (U-Th)/He 定年, 理想矿物应是具备适度放射性核素 (几十个 $\mu\text{g/g}$) 且几乎不含包裹体 (Lippolt *et al.*, 1994)。在双目显微镜下选择不含包裹体并排除明显晶型缺陷

的单颗粒尤为重要。然而, 在实际测试中, 无论是反射光还是透射光下, 都难以确保矿物完全不含包裹体, 尤其是微米级包裹体, 需借助电子显微镜或裂变径迹轴质不均一图像才能加以识别。因此, 测年中将不可避免的产生大量“无母体 ^4He ” (Parentless ^4He), 对结果影响极大。Stockli and Farleg (2004) 尝试在 125 倍偏光镜下挑选磷石, 但由于磷石本身透明度较低且表面不平整, 排查包裹体比磷灰石更难。在他们获得的 52 个单颗粒磷石 (U-Th)/He 年龄中 (2~94 Ma), 仍有 5 个年龄异常偏老 (165、110、107、372 及 1 800 Ma)。包裹体在锆石、褐帘石及独居石中甚为普遍, 锆石 U、Th 含量高至 $5\,000 \times 10^{-6}$, 独居石 Th 含量包裹体可占至 30% (Howie *et al.*, 1992)。在正交偏光镜下结合背散射电子探针图像, 用 EDS 能谱识别包裹体或许是行之有效的方法之一。部分包裹体中 ^4He 在真空加热过程中被释放, 而磷灰石中硅酸盐包裹体可溶解于 HNO_3 中, 因此, 在矿物本身 U、Th 含量较高的情况下, 微小包裹体对结果的影响并非很大 (House *et al.*, 1997), 这一结论也得到了 Vermeesch *et al.* (2007) 所提出的模型验证 (图 3)。

假设球状磷灰石晶体半径为 R_a , 其包含半径为 R_i 的球型包裹体, 若包裹体比磷灰石颗粒小 10 倍, 即 $R_i = R_a/10$, 则其横截面积对应小 100 倍 ($A_i = A_a/100$), 包裹体体积随之小 1 000 倍 ($V_i = V_a/1\,000$)。换言之, 当磷灰石中铀含量极低 (1×10^{-6}) 时, 包裹体的铀浓度需要增加 1 000 倍 (达 $1\,000 \times 10^{-6}$) 才能产生等量的 ^4He , 该结论亦适用于非球面几何体。比

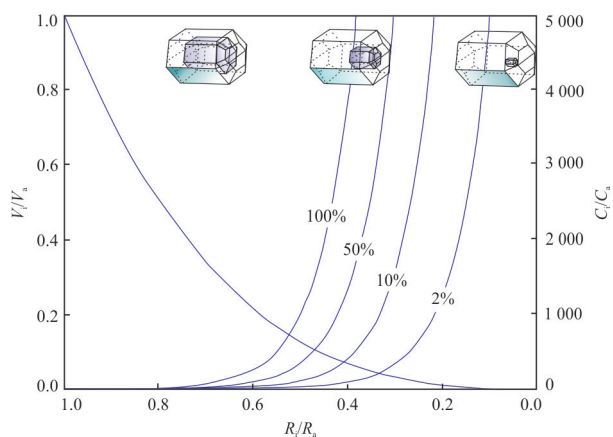


图3 磷灰石包裹体粒径变化对矿物中 ^4He 贡献趋势(根据 Vermeesch *et al.*, 2007 修改)

Fig.3 Apatite inclusions effect on the contribution of ^4He trendgram (after Vermeesch *et al.*, 2007)

如,铀含量为 10×10^{-6} 的棱柱形磷灰石,如果包裹体长宽高分别只占磷灰石的 1%,那么该包裹体体积仅为磷灰石颗粒的百万分之一.即使假设整个包裹体都是纯铀质的极端情况,其 ^4He 含量仅增加 10%.通常情况下,粒径约 100 μm 的磷灰石其 U 浓度约为 10×10^{-6} ,锆石中的包裹体 U、Th 浓度常介于 $100 \times 10^{-6} \sim 1\,000 \times 10^{-6}$ (最高可达 $5\,000 \times 10^{-6}$) 之间.独居石 Th 含量略高,因此,除非矿物中含有较多包裹体,否则亚-微米级的包裹体并非放射成因 ^4He 的主要来源,粒径较大的包裹体才是影响定年结果的主要因素.

3.2 矿物粒径

首先,矿物中的子体同位素会随矿物扩散域边界发生一定量丢失,Durango 磷灰石扩散实验表明,不同粒径样品活化能相同,但扩散系数不同,因此粒径小的晶体更容易通过扩散损失更多 ^4He ,导致年龄偏小.不同粒径的矿物颗粒其计时起始时间存在差异,较大部分保留区驻留时间放大了这种差异.由于磷灰石的扩散域为晶粒本身,随着晶粒尺寸的减小,扩散系数随之增大,导致不同尺寸颗粒的封闭温度也不同,例如,粒径 70~90 μm 的磷灰石封闭温度约为 70 $^{\circ}\text{C}$ (Farley, 2000),在实际测试中,应尽量挑选粒径相似的颗粒,以提高年龄测定的准确性.其次,不同粒径的矿物对 ^4He 保存能力存在差异.磷灰石和榍石矿物扩散域随晶体大小变化,这意味着特定温度下,较大晶体会比较小晶体更易保留 ^4He ,产生偏老的年龄.晶体尺寸对于年龄的影响很大程度上取决于地质体所经历的热历史,对于快速冷却过程,He 年龄代表较窄温度范围内的冷却时间,此时粒径大小可以忽略.在缓慢冷却过程中, ^4He 产生缓慢,或者在部分保留区滞留时间较长.因此,年龄一定程度上取决于因晶体尺寸变化引起的 ^4He 损失比例.理论上,年龄亦会受扩散率微小变化的影响,这可能是由未知的成分效应引起.Reiners and Farley (2001) 研究怀俄明州中北部 Bighorn 山脉磷灰石样品时,揭示出 ^4He 年龄与晶体大小之间的正相关关系,即(1)磷灰石 ^4He 保存能力受制于晶体大小,晶体越大越易保存 ^4He ,在 30~65 $^{\circ}\text{C}$ 温度区间内,粒径较大样品(90 μm)与较小样品(30 μm)之间的年龄差异最大.(2)矿物粒径差异引起的年龄偏差随温度的增加而增大.实际上,构造活动频繁的造山带样品在中-低温等温带附近滞留较长时间,年龄易受粒径影响,粒径大小与年龄的相关关系可用于研

究地表岩石剥蚀速率、时间及地形地貌演化等.

3.3 α 粒子射出效应

铀系元素 ^{238}U 、 ^{235}U 、 ^{232}Th 衰变后的 α 粒子(即 ^4He)具备 4~8 MeV 初始动能,并在相对于母核位置运动一定距离后停止,该距离称为 α 停止距离(α -stopping distance),介于 11~34 μm (Farley *et al.*, 1996),是(U-Th)/He 定年中影响年龄结果准确度的重要因素之一.对于高 U-Th 矿物(如榍石、锆石), α 停止距离较长会造成 α 粒子逃逸到其他矿物晶体外部,造成 ^4He 丢失.矿物外紧邻其边缘的放射性元素也可射出 α 粒子,弹射进入晶体内部,形成过剩 ^4He .一般情况下,矿物晶体中 U、Th 含量远高于周围介质,因此对其年龄的影响相对较小.

当母、子体同位素分布不均时, α 粒子的射出效应使得年龄难以解释.停止距离大小主要取决于衰变能量、矿物密度和晶体组分.例如, ^{238}U 、 ^{235}U 、 ^{232}Th 衰变的 α 粒子停止距离依次增大,从磷灰石(密度为 3.2 g/cm^3)到榍石(密度为 3.6 g/cm^3)、再到锆石(密度为 4.4 g/cm^3), α 粒子平均停止距离随之变小(Ketcham *et al.*, 2011)(表 3).

表 3 中同一矿物的 α 粒子停止距离略有不同.Ketcham *et al.* (2011) 认为,停止距离是能量的非线性函数,基于整个衰变体系中单粒子能量来计算平均停止距离,结果比 Farley *et al.* (1996) 获得结果稍小约 1.5 μm ,其对应 F_T 值相差 1.0%~1.5%.

由于 α 粒子射出效应,所获得的年龄并非样品实际年龄,因此需引入校正参数 F_T ,表示晶体中实际保存的 ^4He 量和理论上保存的 ^4He 总量(包括射出的 ^4He)之间比值,目前已有多种年龄校正模型:

(1) Farley *et al.* (1996) 提出直接对原始年龄进行校正:

$$t_{\text{Corrected-Age}} = t_{\text{Measured-Age}} / F_T, \quad (1)$$

其中, $t_{\text{Measured-Age}}$ 为计算得到的 ^4He 年龄, $t_{\text{Corrected-Age}}$ 表示校正的 ^4He 年龄.该模型被称为均匀球模型或等比表面积模型(晶体表面积与体积的比值),模型假设球体内部 U、Th 含量分布均匀且无外界 α 粒子植入,此时校正因子 F_T 为:

$$F_T = 1 - \frac{3S}{4R} + \frac{S^3}{16R^3}, \quad (2)$$

其中, S 为 α 粒子的停止距离, R 为均匀球半径.由此可知 F_T 值主要取决于半径 R ,若选择较大粒径矿物测年, α 粒子射出效应的影响会减少.

对于均匀球半径 R 远大于停止距离 S 的球体来说,上式可简化为:

表 3 (U-Th)/He 测年主要矿物中各放射性元素产生 α 粒子的停止距离

Table 3 Mean stopping distances of α particles produced from the U, Th and Sm decay chains in several minerals used for (U-Th)/He dating

矿物	密度 (g/cm ³)	平均停止距离(μm)				参考文献	
		²³⁸ U	²³⁵ U	²³² Th	¹⁴⁷ Sm		
磷灰石	3.20	18.81	21.80	22.25	5.93	Ketcham <i>et al.</i> , 2011	
锆石	4.65	15.55	18.05	18.43	4.76		
楣石	3.53	17.46	20.25	20.68	5.47		
独居石	5.26	16.18	18.74	19.11	4.98		
磷钇矿	4.75	15.20	17.63	17.99	4.68		
金红石	4.25	15.30	17.76	18.14	4.77		
磁铁矿	5.18	13.97	16.16	16.49	4.51		
赤铁矿	5.26	13.59	15.72	16.04	4.39		
针铁矿	4.28	15.54	18.00	18.38	4.95		
重晶石	4.50	18.14	21.05	21.50	5.54		
磷灰石	--	19.68	22.63	22.46	--		Farley <i>et al.</i> , 1996
锆石	--	16.97	19.64	19.32	--		
楣石	--	18.12	21.01	20.68	--		

$$F_T = 1 - \left(\frac{S}{4}\right)\beta, \quad (3)$$

其中, β 为球体面积与体积的比率(β=3/R).

(2) 上述的校正模型相对比较简单,但在实际测试中,矿物并非简单的均质球体,体表比 β 和 α 粒子停止距离控制着矿物 ⁴He 的保存. Farley (2002) 对先前的 α 粒子射出效应校正模型进行拓展,提出 F_T 取 U、Th 校正因子的加权平均:

$$F_T = 1 + a_1\beta + a_2\beta^2, \quad (4)$$

其中, a₁ 和 a₂ 根据矿物不同几何形态,通过蒙特蒙特卡洛模拟得到,为 ²³⁸U 和 ²³²Th 衰变系列中 ⁴He 保留在晶体中的比例因子. 根据矿物形态不同,其取值也不同(表 4),如下所示(Farley, 2002; Hourigan *et al.*, 2005):

²³⁵U 和 ²³²Th 衰变能量近似,可使用同一校正参数. 然而, ²³⁸U 的衰变能量低于 ²³²Th, 因此需要对两者之间的校正参数取平均值:

$$F_{T \text{ Mean}} = aF_{T \text{ } ^{238}\text{U}} + (1 - a_{238})F_{T \text{ } ^{232}\text{Th}}, \quad (5)$$

其中, ²³⁸U 衰变生成的 ⁴He 含量可由衰变方程得到,在 (U-Th)/He < 200 Ma 的前提下, a₂₃₈ 可通过下式计算得到: a₂₃₈ = [1.04 + 0.245 (Th/U)]⁻¹ (Wolf *et al.*, 1998).

(3) 上述两种校正方式主要适用于年轻样品,对于较老样品,衰变的非线性增长效应并不能被完全忽略. 为此, Min *et al.* (2003) 利用陨石样品对测量得到的 ⁴He 含量进行 α 校正:

$$^4\text{He}_{\text{Corrected}} = ^4\text{He}_{\text{Measured}} / F_T, \quad (6)$$

表 4 矿物晶体不同几何形态 a₁、a₂ 适用参数

Table 4 Factors a₁ and a₂ for calculating fraction of He retained in crystals from the ²³⁸U and ²³²Th decay series for different assumed crystal geometries

矿物	锆石(四棱柱)		磷灰石(六棱柱)		楣石(四棱柱)	
	a ₁	a ₂	a ₁	a ₂	a ₁	a ₂
²³⁸ U	-4.31	4.92	-5.13	6.78	-4.28	4.37
²³² Th	-5.00	6.80	-5.9	8.99	-4.87	5.61

然后将校正后的 ⁴He 含量与 U、Th 含量一起计算年龄.

(4) 对于非常古老的样品,由于同位素比值的 变化,即 ²³⁵U 相对于 ²³⁸U 变得越来越富集, ²³⁸U 平均 α 粒子停止距离缩短了 15%. Ketcham *et al.* (2011) 提出可分别计算 ²³⁸U、²³²Th 和 ²³⁵U 校正系数,并将晶形拓展到包含 n 棱柱或六棱柱 (n 介于 0~2)、菱面体、三斜晶系等多种形态,分别对应不同校正公式,此处不再赘述.

对母体同位素校正后的计算公式如下:

$$^4\text{He}_{\text{Measured}} = 8F_{T238} ^{238}\text{U} (e^{\lambda_{238}t} - 1) + 7F_{T235} ^{235}\text{U} (e^{\lambda_{235}t} - 1) + 6F_{T232} ^{232}\text{Th} (e^{\lambda_{232}t} - 1) + F_{T147} ^{147}\text{Sm} (e^{\lambda_{147}t} - 1), \quad (7)$$

其中, λ 为各同位素 (²³⁸U、²³⁵U、²³²Th、¹⁴⁷Sm) 的衰变常数; t 为样品积累时间,通常指样品形成到目前的时间.

不论采取何种校正方式均会引入误差,颗粒愈

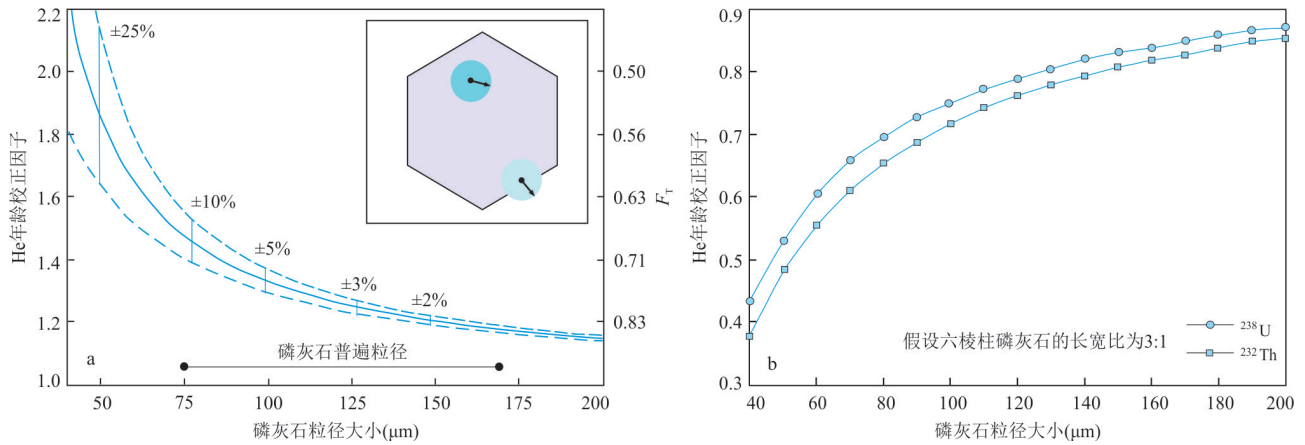


图 4 F_T 校正系数与磷灰石宽度变化关系(修自 Farley, 2002; Ehlers and Farley, 2003)

Fig.4 Correspondence between α -particle correction factor and width of apatite crystal (after Farley, 2000 ; Ehlers and Farley, 2003)

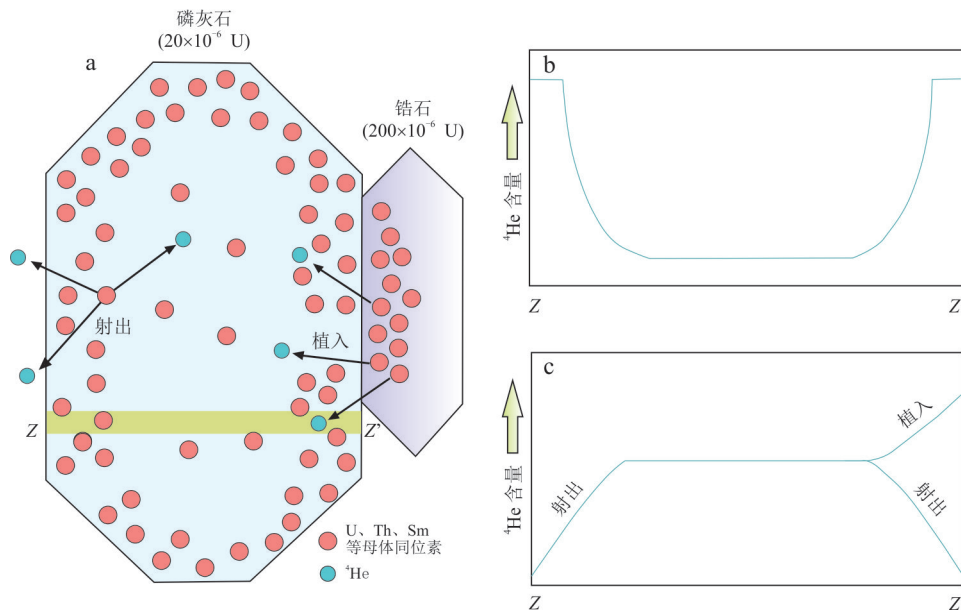


图 5 α 粒子射出和植入效应示意

Fig.5 Schematic diagram of α -particle ejection and implantation

图 a 以磷灰石晶体紧邻锆石晶体为例,磷灰石颗粒边缘为高 U、Th 成分区, Z-Z' 标记为横断面;图 b 表示横断面 Z-Z' 处磷灰石内 ^4He 的分布;图 c 表示在 α 粒子射出效应及周围锆石 ^4He 植入作用下的磷灰石晶体内 ^4He 重新分布情况;据 Chew and Spikings (2015) 修改

小,误差效应愈显著,如粒径 $>75 \mu\text{m}$ 的磷灰石其误差 $<10\%$ (Ehlers and Farley, 2003). 较大颗粒的 F_T 值在 0.8~0.9 的恒定区间内, F_T 值随矿物粒径减小而降低, F_T 值介于 0.65~0.90 时其不确定度较小(图 4). 选择晶形完整、粒径较大的矿物进行测量可最大限度缩小该误差. 长 α 停止距离导致磷灰石晶体外部约 $20 \mu\text{m}$ 的 ^4He 浓度显著耗尽, 在晶体表面附近产生浓度梯度效应(图 5). Farley *et al.* (1996) 和 Ketcham *et al.* (2011) 都曾提出 α 粒子校正模型, 并确定了更详细的基于 U-Th-Sm

分布 α 射出因子 (F_{ZAC}). 然而, 无论是 F_T 还是 F_{ZAC} 校正均未考虑浓度梯度效应对 ^4He 扩散损失的影响.

3.4 ^4He 植入效应

(U-Th)/He 定年的基本假设之一是, 矿物中没有来自寄主岩石或基质的 ^4He 植入. 该假设的成立依赖于相邻矿物的等效铀浓度 (equivalent Uranium, 简称 eU), 对于独居石、锆石、榍石等 eU 高的矿物, 该假设成立; 但对于磷灰石或磁铁矿等 eU 低的矿物, 则该假设不成立. 原因是, 寄主岩石、基质或伴生矿物富集 U、Th 时, 由于 α 粒子停止距离较

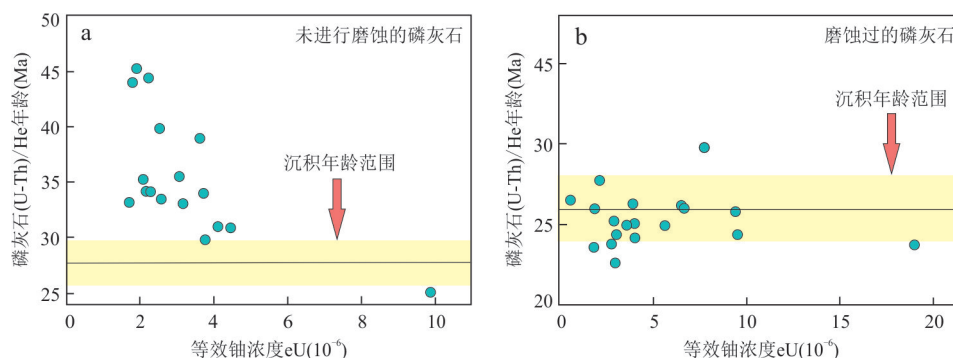


图6 磷灰石(U-Th)/He年龄和等效U浓度关系

Fig.6 Apatite (U-Th)/He date-eU correlations for single-grain analyses

图b为磨蚀掉磷灰石最外层20 μm 厚包壳,据 Spiegel *et al.* (2009)修改

长,外部环境中的 ^4He 会植入到磷灰石内部,造成年龄值偏老.通过对深海沉积物中的碎屑磷灰石研究,前人发现磷灰石中 ^4He 植入导致的eU浓度变化与年龄之间呈负相关.若磨蚀掉磷灰石最外层20 μm 的包壳,此时的(U-Th)/He年龄值等于沉积年龄,这符合矿物内部有 ^4He 植入的假设,能减少 ^4He 植入效应引起的误差(图6)(Spiegel *et al.*, 2009; Flowers *et al.*, 2023b).

对于快速冷却样品,只有高能Th衰变的 α 粒子能在磷灰石内穿透20 μm 以上,此时植入的 ^4He 大部分保存在外部.对于在部分保留带长期滞留的缓慢冷却样品,虽然磨蚀方法不能完全消除 ^4He 植入效应,但仍能显著降低年龄分散性(Gautheron *et al.*, 2012).若 ^4He 植入效应显著,会导致晶体内部扩散明显增强,被磨蚀晶体中保存的过剩 ^4He 比例更高,从而带来年龄误差.磷灰石和锆石的共生模拟研究表明,如果磷灰石只有单一的 ^4He 植入源,其晶体中过剩的 ^4He 比例可达60%以上;而在有多个 ^4He 植入源的情况下, ^4He 含量甚至可以高达250%~300%.值得注意的是,磁铁矿往往伴生磷灰石,其U、Th、Sm浓度(低至 10^{-9} 级别)显著低于周围介质,极易受周围介质 α 粒子植入效应干扰.在磁铁矿(U-Th)/He测年样品的处理和年龄校正中应充分考虑这一点(Min *et al.*, 2006).U、Th、Sm浓度更低的尖晶石(<100 ng/g),其 ^4He 植入效应也不可忽视(Cooperdock and Stockli, 2016).

除毗邻矿物和宿主基质外,尤其是在火山岩中,磷灰石晶体外围若伴生eU浓度极高的铁氧化物和黏土矿物时, ^4He 极易植入磷灰石内部.次生矿物是否会从外部植入 ^4He 到磷灰石内部,主要取决于磷灰石粒径的大小、毗邻矿物eU浓度、磷灰石外

部包壳的厚度及共生矿物的形成时间等诸多因素.这些因素导致磷灰石的He年龄和eU浓度之间会呈现不同相关性.对于缓慢冷却的样品,由于 ^4He 植入效应产生的年龄误差约为8%,如遇磷灰石和锆石共生时,误差会更大.颗粒尺寸、周边介质中 α 放射剂量及锕系元素的种类均会造成 ^4He 植入效应.例如,在富锕系元素花岗岩和沉积岩中,磷灰石的植入效应更为显著.品质铀矿的次生矿物节理、裂隙及晶洞等也会成为 α 粒子的来源.目前,通过单晶粒多次分析、原位激光探针分析、 $^4\text{He}/^3\text{He}$ 阶段升温实验以及颗粒磨蚀裂变径迹分析,都可进行植入效应相关研究(Phillips *et al.*, 2007).

3.5 成分环带

矿物结晶生长中元素供给不均匀,导致锆石、石榴石和磷灰石晶体中常出现U-Th成分环带,其存在会带来以下问题:(1)影响 ^4He 浓度梯度和 ^4He 整体保存率.磷灰石对辐射损伤密度尤为敏感,晶体内部U、Th含量变化会导致 ^4He 扩散速率随之改变(Shuster and Farley, 2009);(2)多重辐射损伤效应导致同位素非均匀扩散;(3) α 粒子校正参数不再适用(Farley *et al.*, 2011).ICP-MS激光剥蚀方法、扫描电镜、电子探针、阴极发光成像、背散射技术及拉曼光谱等技术均可检测到磷灰石成分环带(Jolivet *et al.*, 2003).若样品已进行径迹蚀刻,还可通过表面径迹密度分布差异来评估环带分布特征(Meesters and Dunai, 2002).然而,磷灰石环带对年龄离散度的影响较小,大多数情况下不予考虑(Ault and Flowers, 2012).矿物内部母体同位素变化不可避免,即便是校正后年龄依旧存在一定误差.对存在典型环带的矿物,再沿用常规 α 粒子射出效应模型校正会导致核部富集U、Th的样品年龄“过

老”,而边部富集 U、Th 的样品年龄“过于年轻”.对锆石而言,分带效应是导致年龄结果离散的重要因素,例如,Tardree 凝灰岩锆石自发裂变径迹密度表明,多数样品核部密度高(即 U 含量高),而边缘密度低,强烈 U-Th 分带效应导致 α 校正因子过高,致年龄偏老,其 He 年龄((78.8±7.0) Ma)高于 U-Pb 年龄((58.4±0.7) Ma)(Tagami *et al.*, 2003).

锆石中 ^4He 均匀分布通常只会如下几种情况下成立:(1)U、Th 含量低;(2)缓慢冷却过程中,通过扩散损失 ^4He ;(3)粒子射出效应影响至外围 ~20 μm 区域,上述情况均会导致实验初始阶段表现扩散系数异常低,随后逐渐消失.对于不同粒径的锆石,甚至可清楚地观察到晶粒边缘的 ^4He 耗尽效应(Reiners and Farley, 1999).若 U、Th 含量高,锆石初始阶段的扩散系数随之升高,导致边缘的 ^4He 含量增加(Reiners *et al.*, 2002).背散射、阴极发光成像及激光剥蚀技术证实,Cornucopia-Wallowas 锆石样品中约 30% 的晶体在边缘 1~3 μm 处 U、Th 含量高出 1.5~2.0 倍,尤其在晶体锥尖部位.然而,局部高 U、Th 含量并不能解释其高扩散率的变化,因为即便是 U、Th 含量十分均一的斯里兰卡锆石晶体内部也会呈现显著的扩散率变化.

一般来说,振荡环带或局部环带对于整个矿物内部 ^4He 保存性而言可忽略不计,此时环带对年龄准确度影响较小.真正对其年龄产生显著影响的是核部与边缘的母体同位素比值.假定 U、Th 全部富集在核部至边缘 20 μm 以上区域,此时 F_T 值近乎一致,而若母体同位素全部集中于矿物边缘时, F_T 值取决于矿物晶形和尺寸,约在 0.4~0.5 之间.当 U、Th 富集于矿物核部,矿物实际损失的 ^4He < U、Th 均一分布时的 ^4He 损失,导致 ^4He 整体保存性被低估, F_T 小于实际值,年龄偏老.反之,当 U、Th 富集于矿物边缘,甚至集中于 1~2 μm 区域内时,会导致年龄偏年轻,误差最大可达 25%.此时,亏损带相当于一个 α 粒子的停止距离.若假设四方晶系的模型长、宽分别为 200 μm 和 100 μm ,锥高为 50 μm ,当锆石 U、Th 在边缘富集形成宽约 2~5 μm 环带时,误差最大高达 40%(图 7).此外,在不考虑辐射损伤或特定热历史影响的情况下,对于较小颗粒,母体同位素分带效应的影响更为显著.

假设不考虑浓度剖面及扩散影响,并且未进行环带 F_T 校正的情况下,Hourigan *et al.*(2005)研究了晶粒半径分别为 45 μm (图 8a)、60 μm (图 8b)和

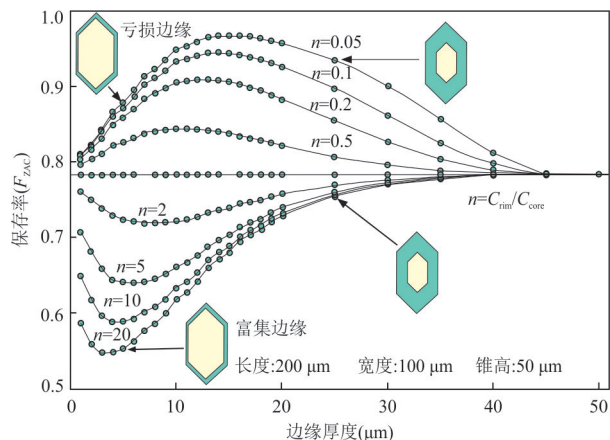


图 7 四方晶系模型的环带宽度变化与 ^4He 保留性相关关系简化图(据 Hourigan *et al.*, 2005)

Fig.7 Zoning-dependent bulk retentivity plots for tetragonal model crystals with rims (concentration step functions) of variable width and degree of enrichment or depletion (after Hourigan *et al.*, 2005)

75 μm (图 8c)球形晶体,在其边缘富集或亏损 U、Th 对年龄准确性的预测模型.显而易见, F_T 的参数偏差对年龄准确性的影响可达 20%~30%.随着晶粒半径的增加,由亏损引起的年龄偏差逐渐减少,而由富集引起的年龄偏差则无明显变化.在天然锆石和磷灰石中,由于多次生长和重溶作用,环带从核部到边缘普遍发育.磷灰石的环带导致其核部和边缘的 U、Th 浓度差异约 2~3 倍,而锆石中浓度差异可高达数量级.

为此,不断有学者提出解决方案.例如,Hourigan *et al.*(2005)提出 U-Th 分带年龄校正模型,该模型可同时适用于球型晶体和双锥棱柱晶体. Bargnesi *et al.*(2016)提出利用 LA-ICP-MS 技术构建母体同位素分布剖面,结合阴极发光(cathodo luminescence, 简称 CL)技术进行联合环带识别,以提高锆石 He 年龄准确度. Spiegel *et al.*(2009)则认为,通过磨蚀掉磷灰石晶体最外层 20 μm 厚的包壳,可解决成分环带带来的校正偏差.近年来,激光微区剥蚀技术的兴起不仅规避了环带问题,还能够在获取浓度剖面时可同步获取矿物内部的微量元素信息,尤其适用于碎屑磷灰石的 (U-Th)/He 定年(Pickering *et al.*, 2020).对传统方法,可选择将矿物抛光后再识别环带或增加单个样品的测试量.然而,由于环带变化不规律,上述方法效果甚微.采用核部到边缘激光剥蚀坑中深度剖面来表征 U-Th 特征,再将深度剖面转化为对应分带模型后进行单颗粒 α 投影校

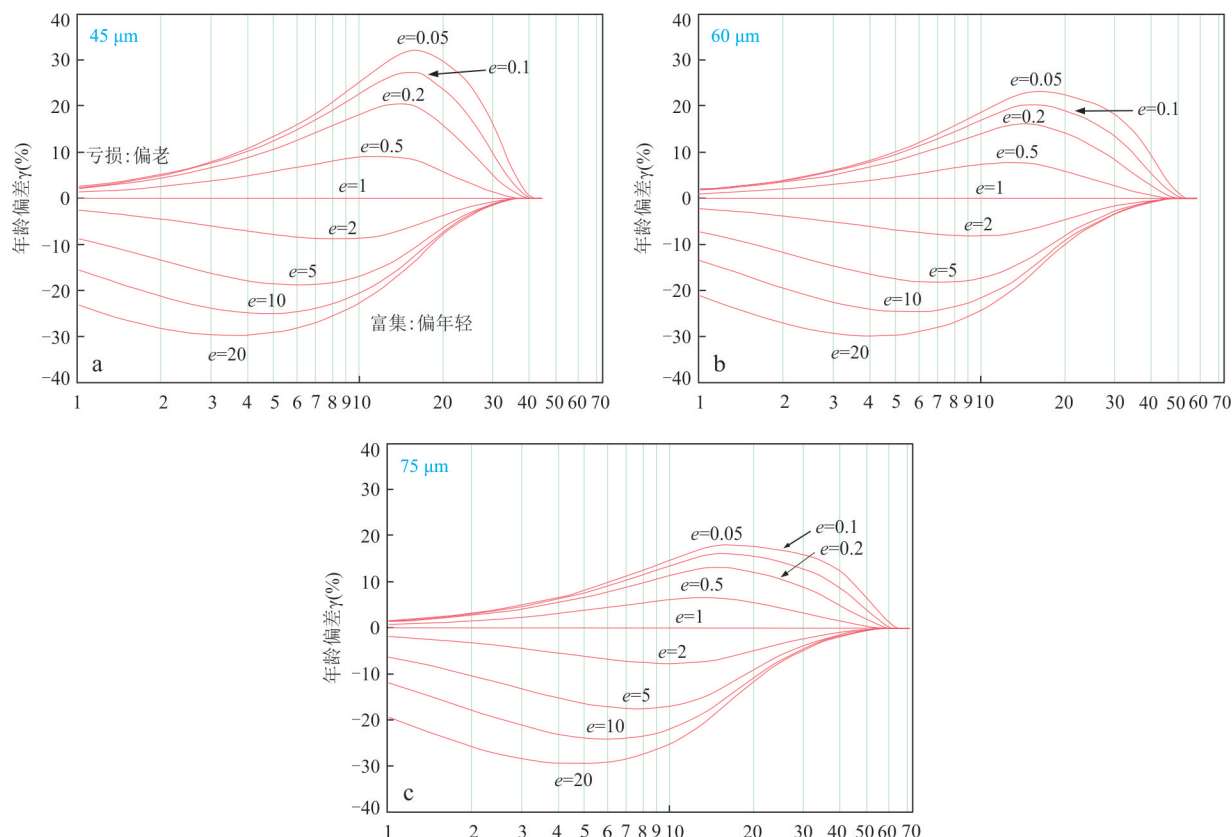


图 8 不同粒径矿物边缘富集/亏损 U、Th 的球形晶体对 (U-Th)/He 年龄准确度的影响关系(据 Hourigan *et al.*, 2005 修改)
 Fig. 8 He age bias plots for spherical model crystals with rims (concentration step functions) of variable thickness and degree of enrichment or depletion (after Hourigan *et al.*, 2005)

正的方式,或许值得尝试(Hourigan *et al.*, 2005).

3.6 辐射损伤

辐射损伤(radiation damage),又称 α 粒子反冲损伤,指矿物中母体核素发生放射性衰变时释放的能量通过晶格传递,致使原子发生位移和碰撞,产生原子缺失、局部电荷不平衡、晶格混乱及矿物非晶质蜕变等一系列损伤.这些损伤可表现为围绕高 U-Th 包裹体的多色晕、 α 粒子反冲径迹、移动裂变碎片产生径迹、由在亚稳态高能缺陷位置捕获电子而产生的发光和电子自旋特征等.随着时间的推移,辐射损伤会发生退火效应,退火程度取决于晶体初始辐射损伤密度、退火温度及热事件持续时间等因素(Ault *et al.*, 2015).

3.6.1 磷灰石辐射损伤 磷灰石退火动力学研究表明,假设冷却速率为 $10\text{ }^\circ\text{C}/\text{Ma}$, 粒径 $70\text{ }\mu\text{m}$ 的磷灰石封闭温度约 $70\text{ }^\circ\text{C}$, 而辐射损伤效应会导致磷灰石 He 扩散参数及其封闭温度变化(Farley, 2000). 磷灰石中的辐射损伤源自于 U-Th-Sm 衰变的 α 反冲损伤和 ^{238}U 自然裂变损伤, 损伤密度取决于 U、Th、Sm 浓度以及损伤-退火速率, 其中损伤-退火速率

随晶体化学成分和热历史变化. Shuster *et al.* (2006) 指出, 磷灰石中 ^4He 扩散对晶体结构的辐射损伤分数十分敏感, 多次阶段升温实验亦证实 ^3He 、 ^4He 扩散率与磷灰石中 ^4He 浓度呈负相关, 损伤区域 ^4He 原子被捕获. 损伤积累和退火效应造成其 ^4He 保存性随时间变化, 遭受辐射损伤的矿物产生的晶格缺陷会阻止 ^4He 的扩散, 从而提高矿物在相同环境下对 ^4He 的保存能力. Shuster *et al.* (2006) 利用 $[^4\text{He}]$ 作为辐射损伤衡量指标, 在 Farley (2000) 基础上提出磷灰石 ^4He 扩散俘获模型(trapping model). 该模型的实质是通过扩散作用在晶格中迁移的原子会遇到辐射损伤引起的空缺或无序区域, 这个区域在能量上有利于 ^4He 原子停留. ^4He 原子从这些“陷阱”迁移到晶格中需要额外的活化能 E_t , 图 9a 和 9b 分别表示无放射损伤晶体和放射损伤晶体内 ^4He 原子从某一位置被射出后运移一定距离. 图 9c 表示 ^4He 原子在辐射损伤效应积累晶体内 ^4He 原子从某一位置被射出后的运移距离. 图 9 示意了 3 种不同情况下的有效活化能变化, 在无辐射损伤情况下, ^4He 原子的初始动能为其提供运动的能量; 在放射损伤晶体内, ^4He

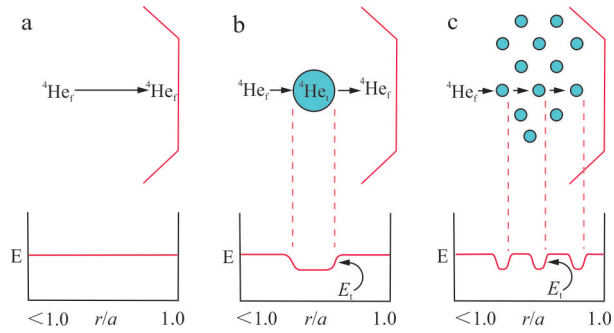


图9 辐射损伤对 ^4He 扩散动力学的影响示意(据 Shuster *et al.*, 2006)

Fig.9 Schematic model of the influence of radiation-damage traps on ^4He diffusion (after Shuster *et al.*, 2006)

r 为穿过半径为 a 的球面距离, $r/a=1$ 对应于晶体表面位置, He_r 表示未损伤晶体内射出的He原子, He_t 为损伤位置上被俘获的He原子, E_a 为通过晶体内完全没有辐射损伤区域的体扩散活化能, E_t 是氦原子克服晶格缺陷阻力逃离未损伤区域所需能量

初始动能 E_a 减去克服晶格缺陷的阻力 E_t 后为He原子提供能量;在辐射损伤积累的晶体内部, ^4He 原子的初始动能 E_a 减去 n 倍克服晶格缺陷阻力能量 E_t 后为其提供能量.因此,晶格缺陷成为阻碍 ^4He 原子扩散运移的障碍,可提高 ^4He 的保存能力.

等效铀浓度($eU = [U] + 0.235\text{Th}$ 或 $eU = [U] + 0.234 \times [\text{Th}] + 0.0046 \times [\text{Sm}]$)(Guenther *et al.*, 2013)和 $[^4\text{He}]$ (α 粒子浓度)(Shuster *et al.*, 2006)两个指标可用于反映矿物的辐射损伤程度, eU 高或 $[^4\text{He}]$ 高的晶体中对 ^4He 保存性更高.

实际上, eU 并非完全意义上的 ^4He 含量,它只是作为经历相同热历史晶粒之间对比辐射损伤的衡量参数.对于任何给定热历史的地质体来说, eU 较高的磷灰石封闭温度较高,($U\text{-Th}$)/He也会较

老.因此,磷灰石He丢失的动力学机制随热历史不同而变化.然而,由于热历史的差异,磷灰石热历史和 eU 之间关系亦不相同(图10).从图10可以看出,快速冷却样品中, eU 最低时的有效封闭温度为 57°C , eU 最高时封闭温度为 65°C ,其值均小于Durango磷灰石封闭温度(72°C).随着冷却速率降低,不同 eU 浓度磷灰石封闭温度越来越分散,表明辐射损伤影响氦扩散持续时间较长.在快速冷却条件下,磷灰石通过部分保留带速度极快,其遭受辐射损伤效应比Durango磷灰石少,因此其有效封闭温度低于Durango磷灰石.相反,在较低冷却速率时,随着辐射损伤积累和扩散率显著降低,磷灰石有效封闭温度高于Durango磷灰石.

图10显示了Shuster *et al.*(2006)计算的 ^4He 部分保留带与Durango磷灰石相似.在较低温度下辐射损伤效应增强,其 ^4He 保存性接近甚至是超过Durango磷灰石.相反,在较高温下,低辐射损伤磷灰石对 ^4He 的保留性较低.在较低温度下,辐射损伤效应增强,因此其 ^4He 保存性接近甚至是超过Durango磷灰石(图10a).对于 eU 含量居中的磷灰石,将 ^4He 部分保留带定义为 $10\% \sim 90\%$ 之间,温度在 $38 \sim 54^\circ\text{C}$ 之间,而Durango磷灰石则是在 $34 \sim 65^\circ\text{C}$ 之间, eU 差异造成其部分保留带之间近 20°C 的差异,($U\text{-Th}$)/He年龄随之变化(图10b).

以 ^4He 浓度作为辐射损伤衡量指标并非理想选择,因为辐射损伤累积可随时间推移发生退火,而蚀刻径迹也是辐射损伤的一种形式,二者都依赖于时间和温度,但其动力学机制并不相同.Shuster and Farley(2009)对比了俘获模型中 ^4He 扩散率预测值与直接采用中子轰击造成的辐射损伤对 ^4He 扩散率

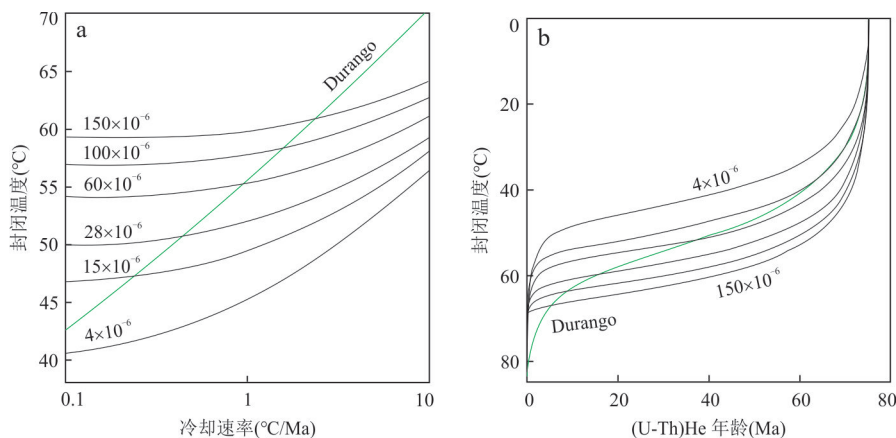


图10 不同等效铀浓度对应的Durango磷灰石的封闭温度及($U\text{-Th}$)/He年龄变化(据 Shuster *et al.*, 2006 修改)

Fig.10 Closure temperature (T_c) for Durango apatite and grains with varying eU concentrations (after Shuster *et al.*, 2006)

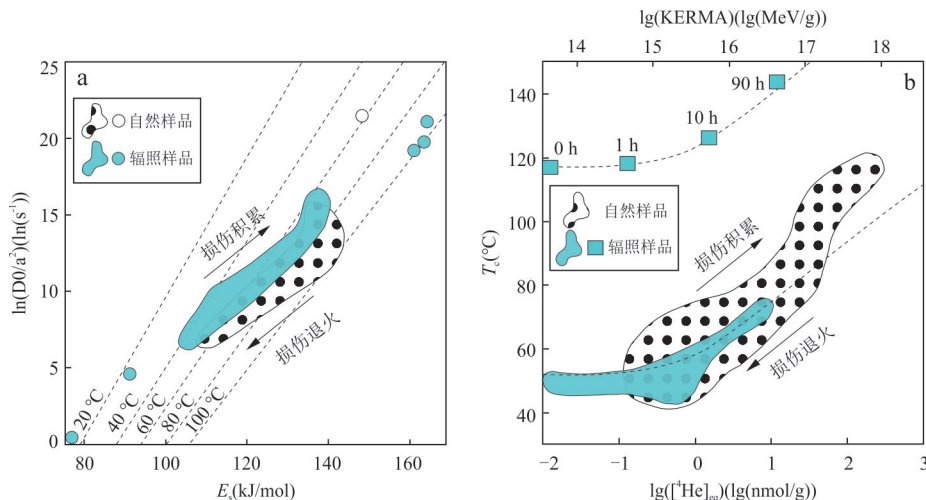


图 11 人工辐照磷灰石和天然磷灰石扩散参数对比(据 Shuster and Farley, 2009)

Fig.11 Kinetic parameters of natural and artificially irradiated samples (after Shuster and Farley, 2009)

的影响,结果表明辐射损伤可阻滞磷灰石的⁴He扩散,但热退火可以逆转该过程.自然和人为损伤的积累对扩散系数(即封闭温度)具等效影响,通过加热实现辐射损伤退火可消除损伤并导致封闭温度降低,即磷灰石⁴He扩散动力学将随时间和温度发生变化(图11).

天然矿物及人工诱导辐射损伤的矿物均遵循相似的动力学参数,在核反应堆中暴露于1~100 h条件下的天然磷灰石,其辐照增加了活化能(E_a)和扩散频率因子(D_0/a^2),使封闭温度升高(图11a).辐照矿物内⁴He产生和扩散损失近乎平衡,中子辐照后⁴He浓度(8.7 nmol/g)近似等于初始⁴He浓度(8.2 nmol/g),即在等效 $[^4\text{He}]$ 条件下,中子辐照90 h后样品的封闭温度相差约15 °C,表明辐射损伤控制了⁴He保留率(图11b).因为辐射损伤是⁴He扩散率的控制参数,所以样品损伤程度的量化方法值得探讨.Shuster and Farley(2009)注意到样品中裂变径迹长度与(U-Th)/He封闭温度之间呈良好相关性,因此径迹长度或可代表与退火相关的时间-温度综合效应,用来表征辐射损伤程度.然而,绝大多数的晶格缺陷可能是由 α 衰变后重核反冲引起,并且反冲径迹体积比裂变径迹大的多.因此,反冲径迹才是引发⁴He扩散率变化的主要因素.据此,裂变径迹长度并非辐射损伤程度的理想表征,因为只有历经简单热历史的样品才可能出现单峰径迹长度,绝大多数情况下,径迹分布反映的是样品经历了多阶段径迹退火和热历史过程.此外,自发径迹仅由²³⁸U生成,而 α 损伤则同时来源于²³⁵U和²³²Th.基于此,Flowers *et al.*(2009)引入有效裂变径迹密度

(effective spontaneous fission-track density,简称 $e\rho_s$,单位 tracks/cm²)概念作为辐射损伤的衡量指标.

辐射损伤使得磷灰石(U-Th)/He数据解释更加复杂,即使经历相同热历史条件,不同颗粒的⁴He损失程度亦不相同,导致封闭温度存在差异.多种模型的提出为辐射损伤的评估和量化提供了可行的方法.辐射损伤积累与退火模型(radiation damage accumulation and annealing model,简称RDAAM)关注热历史相同但eU浓度不同样品的热史恢复.该模型假设磷灰石的辐射损伤效应主要由 α 反冲损伤引起,不考虑磷灰石中 α 反冲及裂变引起损伤退火速率的不同.然而,在裂变径迹对退火的抵抗力低于 α 反冲损伤的情况下,这一假设可能会过度估计损伤退火速率,导致(U-Th)/He年龄偏低(Flowers *et al.*, 2009).He捕获模型(He trapping model,简称HeTM)是矿物内部不存在辐射损伤的动力学预测模型.该模型假定 α 衰变诱发的晶格缺陷体积分数与 α 粒子(⁴He)浓度成正比.在温度足够低时,捕获模型认为辐射损伤开始积累.较之于eU低的磷灰石,那些eU较高的磷灰石会积累更多的损伤缺陷,其封闭温度也更高.辐射损伤对⁴He扩散影响较大,在典型磷灰石eU分布区间内,封闭温度变化幅度可能相差几十摄氏度.因此,从Durango磷灰石动力学预测得到的时间-温度路径与由⁴He捕获模型产生的(U-Th)/He年龄得到的之间往往存在很大差异.对于某些热过程,辐射损伤的影响表现为(U-Th)/He年龄与eU之间呈正相关关系(Shuster *et al.*, 2006; Flowers *et al.*, 2007).利用这一特性,可以通过eU浓度范围和对应的封闭温度

范围获取热历史. 这种方法与 (U-Th)/He 数据中的年龄-粒径-尺寸相关性关系以及裂变径迹方法中 F/Cl 与年龄关系有着异曲同工之处. 前人对科罗拉多高原 (Flowers *et al.*, 2007, 2008) 及加拿大地盾 (Flowers *et al.*, 2009) 样本的研究亦显示年龄和 eU 浓度之间的密切相关性. α 损伤退火模型 (Alpha-damage annealing model, 简称 ADAM) 摆脱了 α 反冲损伤退火速率与裂变径迹退火相关性假设. 该模型采用实验控制损伤退火和 ^4He 扩散动力学数据, 校准经验关系来量化退火效应, 在 α 反冲损伤退火和 ^4He 扩散率之间提供更直接的关联 (Willett *et al.*, 2017).

3.6.2 锆石辐射损伤 天然锆石氦扩散率受晶体控制, 且具显著各向异性, 意味着不同晶体形态的锆石 ^4He 封闭温度不同 (200~160 °C) (Anderson *et al.*, 2020). U、Th 的衰变破坏了矿物晶格、增强了锆石对化学变化的敏感性, 并影响包括其他惰性气体在内的衰变产物的保留率. 锆石内 eU 浓度高达 $\sim 100 \times 10^{-6} \sim 10\,000 \times 10^{-6}$, 损伤剂量可达 $2 \times 10^{18} \alpha/\text{g}$ (Nasdala *et al.*, 2004). 晶体的自我修复需要更高的退火温度, 因此辐射损伤对 ^4He 扩散的影响效应在锆石中尤为显著. 封闭温度是辐射损伤的函数, 可在 210~250 °C 范围内波动. 初始辐射损伤的积累会破坏锆石晶体平行于 *c* 轴方向的扩散路径, 导致扩散系数降低, 从而封闭温度升高. 辐射损伤逐渐积累达到阈值时, 晶格损伤部位开始连接, 扩散系数显著增大, 封闭温度降低. 基于这种特性, 可通过 eU 与年龄的正负相关性来判别锆石辐射损伤程度 (Guenther *et al.*, 2013). 锆石的辐射损伤积累会破坏锆石有序的晶格结构, 或导致矿物发生蜕晶作用. 在体视显微镜平面偏光下, 辐射损伤积累时间足够长的锆石颗粒 (如太古宙和元古代) 会显示出蜕晶作用, 伴随中-高强度的损伤剂量 (Ewing *et al.*, 2003). 由于辐射损伤显著改变锆石扩散性, 辐射损伤对 ^4He 扩散的影响随损伤增加而变化, 存在两个不同扩散行为阶段: 起初锆石 ^4He 扩散系数降低, 封闭温度从 135 °C 增加至 190 °C. 随着辐射损伤接近约 $5 \times 10^{17} \alpha/\text{g}$ 的阈值, 封闭温度下降, 此后锆石达到完全非晶化. 当损伤程度 < 损伤阈值时, eU 与 (U-Th)/He 年龄正相关; 相反, 损伤程度 > 损伤阈值时, eU 与 (U-Th)/He 年龄呈负相关. 这些相关性有助于模拟岩石样品的时间-温度历史, 从而阐明剥露和埋藏过程. 假设锆石的损伤退火机制和锆石裂变径迹

退火类似, 有效 α 剂量可将锆石辐射损伤区分为低和高损伤类型. 当 α 剂量在 $10^{16} \sim 10^{19} \alpha/\text{g}$ 范围内变化, 由于锆石中辐射损伤对 ^4He 扩散率和热敏感性的影响比晶体各向异性大得多, 在 $1.2 \times 10^{16} \sim 1.4 \times 10^{18} \alpha/\text{g}$ 之间, *c* 轴平行方向上测得的频率因子 D_0 降低约 4 个数量级, 导致 ^4He 扩散率急剧下降 (例如, 在 140~220 °C 之间下降 3 个数量级). 当 α 剂量在 $\sim 2 \times 10^{18} \alpha/\text{g}$ 以上时, 活化能降低约 2 倍, 扩散率增加约 9 个数量级, 高达 $8.2 \times 10^{18} \alpha/\text{g}$. 当辐射损伤程度高时, 在更大损伤剂量下, ^4He 扩散率会急剧增加. 假设随着辐射损伤程度增加, 损伤区域相互连接, 增大了扩散系数, 当 α 剂量在 10^{16} 至 $10^{18} \alpha/\text{g}$ 之间时, 锆石 (U-Th)/He 封闭温从 140 °C 增至 220 °C, 随后在此剂量以上急剧下降. 因此, 辐射损伤对于锆石 He 年龄的影响十分显著. 即遭受严重辐射损伤的锆石可能对温度更加敏感, 因此其封闭温度可能低于常规意义上的 180~200 °C. Guenther *et al.* (2013) 试图建立锆石辐射损伤积累退火模型 (zircon radiation damage accumulation and annealing model, 简称 ZRDAAM), 旨在根据每个锆石晶粒测量的 U-Th 含量计算氦扩散率作为温度-历史的函数, 并将其用于区域热历史研究中 (Orme *et al.*, 2016). 然而, 该模型对于高损伤剂量的锆石并不完全适用. Powell *et al.* (2016) 认为 ZRDAAM 模型中假定的增加氦扩散率的损伤阈值可能被高估了. Johnson *et al.* (2017) 指出, 辐射损伤程度高的锆石中 ^4He 保留率要比采用 ZRDAAM 预测的高. 高辐射损伤锆石的 He 年龄可用于限定 50 °C (低于磷灰石 (U-Th)/He 封闭温度) 以下的低温事件. 对美国科罗拉多州中南部缓慢冷却正长岩中的锆石进行辐射损伤和封闭温度相关性分析结果亦证实, ZRDAAM 模型在 $1 \times 10^{18} \sim 4 \times 10^{18} \alpha/\text{g}$ 之间对锆石 He 封闭温度的估计过高 (Anderson *et al.*, 2017).

损伤积累和损伤退火是控制扩散的两个对立过程, 多年来, 不同损伤研究模型侧重点有所不同, 如直接模型 (direct impact model) 侧重于辐射损伤随时间的积累过程 (Gibbons *et al.*, 1972). 渗率模型 (percolation model) 关注随损伤程度增加损伤连通性的变化特性 (Ketcham *et al.*, 2013), ZRDAAM 模型侧重锆石中的 ^4He 损失研究. 无论哪种模型, 都应该在锆石 (U-Th)/He 数据解释中需充分考虑辐射损伤积累效应以及退火随时间和温度变化的特性. 尽管蚀刻径迹可作为锆石辐射损伤退火的指针, 但

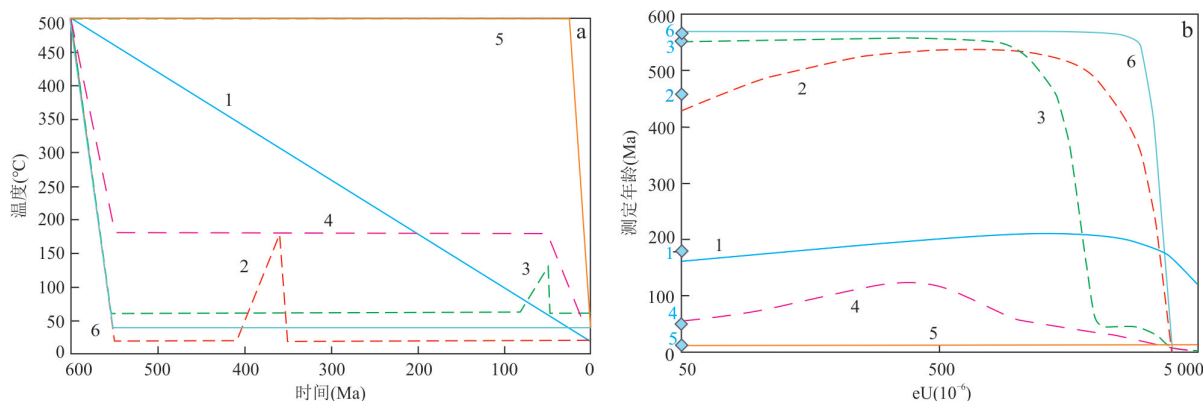


图12 常见热历史路径及对应的年龄-等效U浓度预测关系(据 Guenther *et al.*, 2013)

Fig.12 Model predictions of date-eU correlations for various thermal histories (after Guenther *et al.*, 2013)

辐射损伤退火比蚀刻径迹需更高温度和更长的持续时间.当裂变径迹完全退火时,辐射损伤仅占退火的30%~50%.使用裂变径迹退火会导致对 ^4He 保留率的误判,低、中、高三种不同程度损伤锆石的退火模型可弥补这一缺陷(Ginster *et al.*, 2019).

Guenther *et al.* (2013) 联合 Reiners *et al.* (2004) 的锆石数据,选取 eU 值在 $50 \times 10^{-6} \sim 5000 \times 10^{-6}$ 之间,颗粒半径为 $60 \mu\text{m}$,热历史演化时间为 600 Ma 至今,对常见的 6 种热历史对应的年龄-等效 U 浓度关系进行了模拟(图 12):①缓慢单调冷却;②早期发生冷却,期间发生过热加热事件;③发生冷却后较长时间再次发生热加热事件;④发生冷却以后在部分保留带停滞较长时间;⑤经历较长时间加热时间后发生冷却;⑥冷却后长期处于低温环境(图 12a).其中,⑤、⑥表现出较为平坦的年龄-eU 趋势,是多数锆石的特征,尤其是经历长的路径时间冷却停滞的路径⑥在高 eU 值下出现明显的负相关关系;①、②、③、④热历史则显示,即便是同一样品,也会产生或正或负的相关性;经过部分保留带并缓慢冷却的①显示在相对短的时间内的正相关关系(161~210 Ma),较长时间内同时发生损伤积累和 ^4He 扩散,致使损伤和扩散大体抵消.但当 eU 足够高时,则开始出现轻微负相关关系,而短暂冷却事件往往会造成显著的正、负相关性;②、③的共同特征是都在冷却至 100°C 的低温下之后再次经历加热事件.尽管其锆石损伤程度存在差异,但是都在 eU 达到最高后出现负相关,这与⑥有着类似趋势,即在部分保留带的锆石若其 eU 超过 3500×10^{-6} ,其温度已经很低,此时的矿物中不再保留 ^4He ;不难看出,由于锆石中 ^4He 扩散率与有效 α 剂量之间的关系在临界剂量后发生变化,(U-Th)/He年龄与eU浓度间

相关性主要取决于样品经历的热历史(图 12b).

3.6.3 榧石辐射损伤 榧石 ^4He 扩散实验表明,其 ^4He 扩散遵循各向同性(Cherniak and Watson, 2011),且辐射损伤会增加 ^4He 扩散率,即 ^4He 保留率随辐射损伤增加而急剧下降.辐射损伤退火效应在高损伤样品中更为明显(Baughman *et al.*, 2017;喻顺和田云涛,2023).

当榧石 α 剂量 $>50 \times 10^{16} \alpha/\text{g}$ 时, ^4He 保留性持续下降(图 13a).对于典型榧石的 eU 值($10 \times 10^{-6} \sim 200 \times 10^{-6}$),需要 600~1200 Ma 损伤积累时间来达到损伤阈值.缓慢冷却的样品具备足够的积累时间来达到损伤阈值,因此其年龄与 eU 值呈负相关.榧石的 eU 值低于锆石($500 \times 10^{-6} \sim 2000 \times 10^{-6}$),在相同漫长热历史中,榧石更难以突破损伤阈值,因此在 t - T 演化路径中,榧石比锆石更易进入高温阶段.例如,榧石在较低的 α 剂量下变质程度比锆石高(Ewing *et al.*, 2000).在达到一定剂量阈值后,榧石 ^4He 保存性急剧下降,这和锆石类似.在锆石和榧石的封闭温度与 α 剂量对比图上, α 剂量较低时,两者封闭温度在 $150 \sim 210^\circ\text{C}$ 之间;而当损伤程度较高时(即 α 剂量较高),其封闭温度迅速降低,榧石损伤阈值($\sim 50 \times 10^{16} \alpha/\text{g}$)比锆石($\sim 150 \times 10^{16} \alpha/\text{g}$)低,这可能是由于在 α 反冲或径迹衰变过程中,榧石的损伤域(带)比锆石大,这意味着在较低损伤水平下即可达到渗透阈值,扩散率随之增大.在 ^{238}U 、 ^{232}Th 衰变链中,平均能量 95 keV.榧石产生的 α 反冲停止距离为 29 nm,锆石为 25 nm,榧石径迹长度($19.6 \mu\text{m}$)长于锆石径迹长度($16.7 \mu\text{m}$)(Jonckheere, 2003).尽管榧石和锆石损伤-扩散模式有着相似之处,但它们是否记录相同热历史则还需考虑其 eU 值.在损伤积累时间与 α 剂量变化图上(图

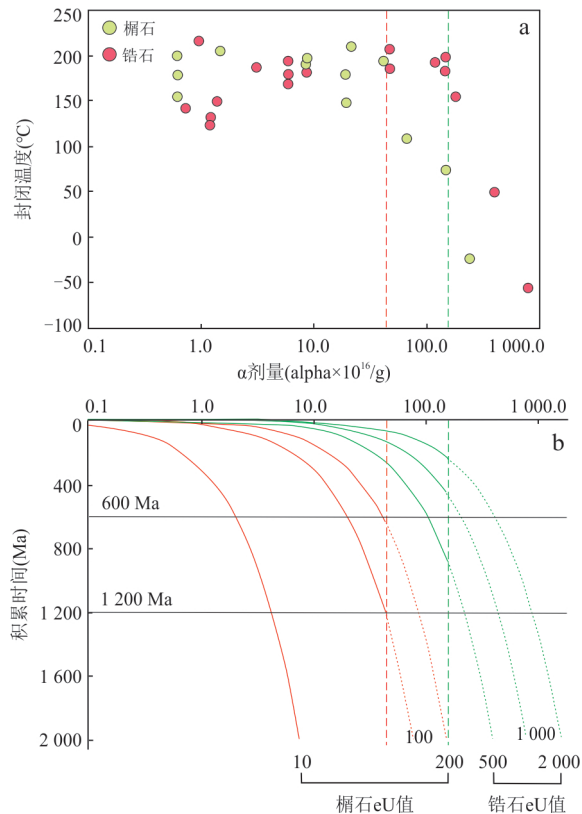


图 13 榍石、锆石封闭温度随 a 损伤剂量变化趋势图(a); 榍石、锆石的损伤积累时间(Ma)、 a 剂量以及 eU 变化关系图(b)(Baughman *et al.*, 2017)

Fig. 13 T_c ($^{\circ}\text{C}$) versus estimated alpha dose ($a \times 10^{16}/g$) for titanites and zircon (a); accumulation time (Ma) versus alpha dose ($a \times 10^{16}/g$) for titanite and zircon of variable eU (b) (modified from Baughman *et al.*, 2017)

13b), 当榍石的 eU 值分别取 10×10^{-6} 、 100×10^{-6} 及 200×10^{-6} 时(红色虚线代表榍石 ^4He 保留率损伤阈值线), ^4He 保留率下降的近似损伤阈值如图 13b 中虚线所示. 因此, 若在 600 Ma 之后榍石 eU 值为 100×10^{-6} , 由于损伤累积不足, 榍石封闭温度仍维持在 150~200 $^{\circ}\text{C}$ 区间; 如需达到足够的损伤, 需要近 1200 Ma 损伤积累时间, 才能达到榍石剂量阈值, 使得其 ^4He 保留率下降. 锆石亦同理, 以 500×10^{-6} 、 1000×10^{-6} 及 2000×10^{-6} 的 eU 值为例(绿色虚线为锆石 ^4He 保留率损伤阈值线), 当锆石 eU 值为 1000×10^{-6} 时, 经过 600 Ma 损伤积累时间后超过其破坏阈值, T_c 降低到 <150 $^{\circ}\text{C}$, 如前所述, 同一岩石中 100×10^{-6} eU 值的榍石由于损伤积累较少, 其封闭温度尚高于 150 $^{\circ}\text{C}$; 图 13 结果表明, 在损伤积累不超过 100 Ma 的情况下, 榍石和锆石年龄都反映低于 150~210 $^{\circ}\text{C}$ 封闭温度区间的冷却事件. 而对于更漫长的热历史

和更长积累时间条件下, 榍石的 ^4He 年龄有可能记录更高温度的(150~210 $^{\circ}\text{C}$)下的冷却事件.

此外, Cherniak and Watson(2011)报道的金红石 ^4He 封闭温度约 150~225 $^{\circ}\text{C}$, 并证实金红石的扩散和锆石类似, 具备各向异性, 扩散优先沿平行于 c 轴的通道发生. 辐射损伤可增强金红石延展性, 其具体损伤机制目前未见报道(Robinson *et al.*, 2019). 对辐射损伤积累机制的认识是 (U-Th)/He 技术应用中数据解释的关键, X 射线衍射、红外和拉曼光谱、原位透射电子显微镜分析, 以及纳米压痕硬度分析都是研究矿物辐射损伤机制的有效方法.

3.7 其他因素

此外, 制约 (U-Th)/He 年龄准确度的因素还有很多. 例如, 磷灰石晶体化学成分或晶格缺陷会影响 ^4He 在磷灰石中的扩散. 磷灰石 ($\text{Ca}_5(\text{PO}_4)_3(\text{F}, \text{OH}, \text{Cl})$) 可发生多种类质同象替换, 其 Cl 可取代 Fe、Mn、Na、Sr 和 Mg 等阳离子, 而 Ca 亦很容易被 La、Ce 等稀土元素所取代. 这些替换可能引起 ^4He 的迁移, 导致封闭温度发生变化. 此外, 目前损伤扩散模型多是基于氟磷灰石的假设研究, 因此一旦化学成分改变, 对 (U-Th)/He 体系就会产生影响. 磷灰石晶格中的微孔和应变位错可以捕获 ^4He 或改变其扩散途径, 导致较高封闭温度(McDannell *et al.*, 2018b). 尽管此前 Wolf *et al.* (1996) 对 Durango 磷灰石的研究中指出, 磷灰石中的 Cl 含量对 ^4He 的影响可以忽略不计, 但近年来的研究表明, 如果 Cl 含量高, 会阻滞辐射损伤退火, 使得损伤效应积累, 捕获更多的 ^4He , 从而导致年龄偏大(Gautheron *et al.*, 2013). 矿物挑选过程不可避免的外力可能导致矿物破碎, 等效半径的计算和 U、Th 均一的假设也因此不再适用, 从而导致年龄偏大或者偏小. ^{147}Sm 衰变生成的 ^4He 约为 0.1%~10%, 其对年龄的影响在 1%~8% 之间, 当 $\text{eU} < 5 \mu\text{g}/g$ 时, 生成的 ^4He 需要测试并参与计算(Fitzgerald *et al.*, 2006).

4 展望与小结

磷灰石、锆石、榍石等副矿物的封闭温度已确定, 其辐射损伤机制研究也已成熟, 是 (U-Th)/He 研究中最常用的矿物. 其他可有效保存 ^4He 的矿物亦可应用于地球科学研究的不同领域, 但仍存在一些值得关注的问题: 如晶体化学性质和辐射损伤对磷钇矿 ^4He 扩散的影响机制研究, 以及适宜大小的磷钇矿的获取; 榍石 ^4He 丢失效应的评估与

量化;萤石裂变径迹与晶体缺陷及微小包裹体之间的有效区分;橄榄石中放射成因 ^4He 的浓度与初始 ^4He 的区分;高温提取 ^4He 时铁氧化物的U丢失问题等,均是未来研究中值得深入探讨的重要问题.多种年龄校正模型的引进大大提高了年龄计算的准确性,但是测试前期包裹体和矿物粒径的影响不可忽视. α 粒子植入效应以及辐射损伤的影响应通过年龄与eU的相关性来判定.成分环带可通过构建母体同位素分布剖面、激光剥蚀坑深度剖面及磨蚀包壳转化成不同校正模型来降低年龄偏差.(U-Th)/He测年技术的发展不仅为区域地质活动的历史和动力学研究提供了可靠依据,还在岩石圈、生物圈、水圈和大气圈等地球各圈层相互作用的研究中展现了广阔前景.

致谢:成文过程中,感谢中国地质科学院地质研究所喻顺副研究员、中国科学院地质与地球物理研究所张斌博士、吴林高级工程师及长安大学陶霓副教授提供的宝贵建议,获益良多.感谢两位匿名审稿人提出的宝贵意见,感谢中国地质大学(北京)洪树炯同学在本文成图过程中提供的帮助.在此一并表示感谢!

References

- Aciego, S. M., Jourdan, F., DePaolo, D. J., et al., 2010. Combined U-Th/He and $^{40}\text{Ar}/^{39}\text{Ar}$ Geochronology of Post-Shield Lavas from the Mauna Kea and Kohala Volcanoes, Hawaii. *Geochimica et Cosmochimica Acta*, 74(5): 1620–1635. <https://doi.org/10.1016/j.gca.2009.11.020>
- Aciego, S., Kennedy, B. M., DePaolo, D. J., et al., 2003. U-Th/He Age of Phenocrystic Garnet from the 79 AD Eruption of Mt. Vesuvius. *Earth and Planetary Science Letters*, 216(1–2): 209–219. [https://doi.org/10.1016/S0012-821X\(03\)00478-3](https://doi.org/10.1016/S0012-821X(03)00478-3)
- Adams, B., Dietsch, C., Owen, L. A., et al., 2009. Exhumation and Incision History of the Lahul Himalaya, Northern India, Based on (U-Th)/He Thermochronometry and Terrestrial Cosmogenic Nuclide Methods. *Geomorphology*, 107(3–4): 285–299. <https://doi.org/10.1016/j.geomorph.2008.12.017>
- Anderson, A. J., Hanchar, J. M., Hodges, K. V., et al., 2020. Mapping Radiation Damage Zoning in Zircon Using Raman Spectroscopy: Implications for Zircon Chronology. *Chemical Geology*, 538: 119494. <https://doi.org/10.1016/j.chemgeo.2020.119494>
- Anderson, A. J., Hodges, K. V., van Soest, M. C., 2017. Empirical Constraints on the Effects of Radiation Damage on Helium Diffusion in Zircon. *Geochimica et Cosmochimica Acta*, 218: 308–322. <https://doi.org/10.1016/j.gca.2017.09.006>
- Anderson, A. J., Hodges, K. V., van Soest, M. C., et al., 2019. Helium Diffusion in Natural Xenotime. *Geochemistry, Geophysics, Geosystems*, 20(1): 417–433. <https://doi.org/10.1029/2018gc007849>
- Ault, A. K., Flowers, R. M., 2012. Is Apatite U-Th Zonation Information Necessary for Accurate Interpretation of Apatite (U-Th)/He Thermochronometry Data? *Geochimica et Cosmochimica Acta*, 79: 60–78. <https://doi.org/10.1016/j.gca.2011.11.037>
- Ault, A. K., Reiners, P. W., Evans, J. P., et al., 2015. Linking Hematite (U-Th)/He Dating with the Microtextural Record of Seismicity in the Wasatch Fault Damage Zone, Utah, USA. *Geology*, 43(9): 771–774. <https://doi.org/10.1130/g36897.1>
- Bargnesi, E. A., Stockli, D. F., Hourigan, J. K., et al., 2016. Improved Accuracy of Zircon (U-Th)/He Ages by Rectifying Parent Nuclide Zonation with Practical Methods. *Chemical Geology*, 426: 158–169. <https://doi.org/10.1016/j.chemgeo.2016.01.017>
- Baughman, J. S., Flowers, R. M., Metcalf, J. R., et al., 2017. Influence of Radiation Damage on Titanite He Diffusion Kinetics. *Geochimica et Cosmochimica Acta*, 205: 50–64. <https://doi.org/10.1016/j.gca.2017.01.049>
- Bidgoli, T. S., Tyrrell, J. P., Möller, A., et al., 2018. Conodont Thermochronology of Exhumed Footwalls of Low-Angle Normal Faults: A Pilot Study in the Mormon Mountains, Tule Springs Hills, and Beaver Dam Mountains, Southeastern Nevada and Southwestern Utah. *Chemical Geology*, 495: 1–17. <https://doi.org/10.1016/j.chemgeo.2018.06.026>
- Blackburn, T. J., Stockli, D. F., Carlson, R. W., et al., 2008. (U-Th)/He Dating of Kimberlites: A Case Study from North-Eastern Kansas. *Earth and Planetary Science Letters*, 275(1–2): 111–120. <https://doi.org/10.1016/j.epsl.2008.08.006>
- Blackburn, T. J., Stockli, D. F., Walker, J. D., 2007. Magnetite (U-Th)/He Dating and Its Application to the Geochronology of Intermediate to Mafic Volcanic Rocks. *Earth and Planetary Science Letters*, 259(3–4): 360–371. <https://doi.org/10.1016/j.epsl.2007.04.044>
- Boyce, J. W., Hodges, K. V., 2005. U and Th Zoning in Cerro de Mercado (Durango, Mexico) Fluorapatite: Insights Regarding the Impact of Recoil Redistribution of Radiogenic ^4He on (U-Th)/He Thermochronology. *Chemical Geology*, 219(1–4): 261–274. <https://doi.org/10.1016/j.chemgeo.2005.03.006>

- org/10.1016/j.chemgeo.2005.02.007
- Boyce, J. W., Hodges, K. V., Olszewski, W. J., et al., 2006. Laser Microprobe (U-Th)/He Geochronology. *Geochimica et Cosmochimica Acta*, 70(12): 3031–3039. <https://doi.org/10.1016/j.gca.2006.03.019>
- Cai, C. E., Chen, H., Shang, W. L., et al., 2020a. Research Progress of Conodont (U-Th)/He Thermochronology. *Advances in Earth Science*, 35(9): 924–932 (in Chinese with English abstract).
- Cai, C. E., Qiu, N., Li, H. L., et al., 2020b. Study of the Closure Temperature of (U-Th)/He in Detrital Zircon Obtained from Natural Evolution Samples. *Science in China (Series D)*, 50(1): 66–78 (in Chinese).
- Calzolari, G., Ault, A. K., Hirth, G., et al., 2020. Hematite (U-Th)/He Thermochronometry Detects Asperity Flash Heating during Laboratory Earthquakes. *Geology*, 48(5): 514–518. <https://doi.org/10.1130/g46965.1>
- Calzolari, G., Rossetti, F., Ault, A. K., et al., 2018. Hematite (U-Th)/He Thermochronometry Constrains Intra-plate Strike-Slip Faulting on the Kuh-E-Faghan Fault, Central Iran. *Tectonophysics*, 728–729: 41–54. <https://doi.org/10.1016/j.tecto.2018.01.023>
- Chang, J., Qiu, N. S., Li, J. W., 2012. Tectono-Thermal Evolution of the Northwestern Edge of the Tarim Basin in China: Constraints from Apatite (U-Th)/He Thermochronology. *Journal of Asian Earth Sciences*, 61: 187–198. <https://doi.org/10.1016/j.jseaes.2012.09.020>
- Cherniak, D. J., Watson, E. B., 2011. Helium Diffusion in Rutile and Titanite, and Consideration of the Origin and Implications of Diffusional Anisotropy. *Chemical Geology*, 288(3–4): 149–161. <https://doi.org/10.1016/j.chemgeo.2011.07.015>
- Chew, D. M., Petrus, J. A., Kamber, B. S., 2014. U-Pb LA-ICPMS Dating Using Accessory Mineral Standards with Variable Common Pb. *Chemical Geology*, 363: 185–199. <https://doi.org/10.1016/j.chemgeo.2013.11.006>
- Chew, D. M., Spikings, R. A., 2015. Geochronology and Thermochronology Using Apatite: Time and Temperature, Lower Crust to Surface. *Elements*, 11(3): 189–194. <https://doi.org/10.2113/gselements.11.3.189>
- Cooperdock, E. H. G., Stockli, D. F., 2016. Unraveling Alteration Histories in Serpentinities and Associated Ultramafic Rocks with Magnetite (U-Th)/He Geochronology. *Geology*, 44(11): 967–970. <https://doi.org/10.1130/g38587.1>
- Cooperdock, E. H. G., Stockli, D. F., 2018. Dating Exhumed Peridotite with Spinel (U-Th)/He Chronometry. *Earth and Planetary Science Letters*, 489: 219–227. <https://doi.org/10.1016/j.epsl.2018.02.041>
- Copeland, P., Watson, E. B., Urizar, S. C., et al., 2007. Alpha Thermochronology of Carbonates. *Geochimica et Cosmochimica Acta*, 71(18): 4488–4511. <https://doi.org/10.1016/j.gca.2007.07.004>
- Cros, A., Gautheron, C., Pagel, M., et al., 2014. ⁴He Behavior in Calcite Filling Viewed by (U-Th)/He Dating, ⁴He Diffusion and Crystallographic Studies. *Geochimica et Cosmochimica Acta*, 125: 414–432. <https://doi.org/10.1016/j.gca.2013.09.038>
- Crowhurst, P. V., Green, P. F., Kamp, P. J. J., 2002. Appraisal of (U-Th)/He Apatite Thermochronology as a Thermal History Tool for Hydrocarbon Exploration: An Example from the Taranaki Basin, New Zealand. *AAPG Bulletin*, 86(10): 1801–1819. <https://doi.org/10.1306/61eadd82-173e-11d7-8645000102c1865d>
- Crowley, P. D., Reiners, P. W., Reuter, J. M., et al., 2002. Laramide Exhumation of the Bighorn Mountains, Wyoming: An Apatite (U-Th)/He Thermochronology Study. *Geology*, 30(1): 27–30. [https://doi.org/10.1130/0091-7613\(2002\)0300027:leotbm>2.0.co;2](https://doi.org/10.1130/0091-7613(2002)0300027:leotbm>2.0.co;2)
- Crowley, Q. G., Heron, K., Riggs, N., et al., 2014. Chemical Abrasion Applied to LA-ICP-MS U-Pb Zircon Geochronology. *Minerals*, 4(2): 503–518. <https://doi.org/10.3390/min4020503>
- Djimbi, D. M., Gautheron, C., Roques, J., et al., 2015. Impact of Apatite Chemical Composition on (U-Th)/He Thermochronometry: An Atomistic Point of View. *Geochimica et Cosmochimica Acta*, 167: 162–176. <https://doi.org/10.1016/j.gca.2015.06.017>
- Dunai, T. J., Roselieb, K., 1996. Sorption and Diffusion of Helium in Garnet: Implications for Volatile Tracing and Dating. *Earth and Planetary Science Letters*, 139(3–4): 411–421. [https://doi.org/10.1016/0012-821x\(96\)00029-5](https://doi.org/10.1016/0012-821x(96)00029-5)
- Ehlers, T. A., Farley, K. A., 2003. Apatite (U-Th)/He Thermochronometry: Methods and Applications to Problems in Tectonic and Surface Processes. *Earth and Planetary Science Letters*, 206(1–2): 1–14. [https://doi.org/10.1016/s0012-821x\(02\)01069-5](https://doi.org/10.1016/s0012-821x(02)01069-5)
- Evans, N. J., Byrne, J. P., Keegan, J. T., et al., 2005. Determination of Uranium and Thorium in Zircon, Apatite, and Fluorite: Application to Laser (U-Th)/He Thermochronology. *Journal of Analytical Chemistry*, 60(12): 1159–1165. <https://doi.org/10.1007/s10809-005-0260-1>
- Evenson, N. S., Reiners, P. W., Spencer, J. E., et al., 2014. Hematite and Mn Oxide (U-Th)/He Dates from the Buckskin-Rawhide Detachment System, Western Arizona: Gaining Insights into Hematite (U-Th)/He Sys-

- tematics. *American Journal of Science*, 314(10): 1373–1435. <https://doi.org/10.2475/10.2014.01>
- Ewing, R. C., Meldrum, A., Wang, L., et al., 2000. Radiation-Induced Amorphization. *Reviews in Mineralogy and Geochemistry*, 39(1): 319–361. <https://doi.org/10.2138/rmg.2000.39.12>
- Ewing, R. C., Meldrum, A., Wang, L., et al., 2003. Radiation Effects in Zircon. *Reviews in Mineralogy and Geochemistry*, 53(1): 387–425. <https://doi.org/10.2113/0530387>
- Fanale, F. P., Kulp, J. L., 1962. The Helium Method and the Age of the Cornwall, Pennsylvania Magnetite Ore. *Economic Geology*, 57(5): 735–746. <https://doi.org/10.2113/gsecongeo.57.5.735>
- Farley, K. A., 2000. Helium Diffusion from Apatite: General Behavior as Illustrated by Durango Fluorapatite. *Journal of Geophysical Research: Solid Earth*, 105(B2): 2903–2914. <https://doi.org/10.1029/1999jb900348>
- Farley, K. A., 2002. (U-Th)/He Dating: Techniques, Calibrations, and Applications. *Reviews in Mineralogy and Geochemistry*, 47(1): 819–844. <https://doi.org/10.2138/rmg.2002.47.18>
- Farley, K. A., 2007. He Diffusion Systematics in Minerals: Evidence from Synthetic Monazite and Zircon Structure Phosphates. *Geochimica et Cosmochimica Acta*, 71(16): 4015–4024. <https://doi.org/10.1016/j.gca.2007.05.022>
- Farley, K. A., Shuster, D. L., Ketcham, R. A., 2011. U and Th Zonation in Apatite Observed by Laser Ablation ICPMS, and Implications for the (U-Th)/He System. *Geochimica et Cosmochimica Acta*, 75(16): 4515–4530. <https://doi.org/10.1016/j.gca.2011.05.020>
- Farley, K. A., Stockli, D. F., 2002. (U-Th)/He Dating of Phosphates: Apatite, Monazite, and Xenotime. *Reviews in Mineralogy and Geochemistry*, 48(1): 559–577. <https://doi.org/10.2138/rmg.2002.48.15>
- Farley, K. A., Wolf, R. A., Silver, L. T., 1996. The Effects of Long Alpha-Stopping Distances on (U-Th)/He Ages. *Geochimica et Cosmochimica Acta*, 60(21): 4223–4229. [https://doi.org/10.1016/s0016-7037\(96\)00193-7](https://doi.org/10.1016/s0016-7037(96)00193-7)
- Feng, Q. Q., Qiu, N. S., Chang, J., et al., 2018. Tectonothermal Evolution of Fangshan Pluton: Constraints from (U-Th)/He Ages. *Earth Science*, 43(6): 1972–1982 (in Chinese with English abstract).
- Fitzgerald, P. G., Baldwin, S. L., Webb, L. E., et al., 2006. Interpretation of (U-Th)/He Single Grain Ages from Slowly Cooled Crustal Terranes: A Case Study from the Transantarctic Mountains of Southern Victoria Land. *Chemical Geology*, 225(1–2): 91–120. <https://doi.org/10.1016/j.chemgeo.2005.09.001>
- Flowers, R. M., Ketcham, R. A., Enkelmann, E., et al., 2023b. (U-Th)/He Chronology: Part 2. Considerations for Evaluating, Integrating, and Interpreting Conventional Individual Aliquot Data. *GSA Bulletin*, 135(1–2): 137–161. <https://doi.org/10.1130/b36268.1>
- Flowers, R. M., Ketcham, R. A., Shuster, D. L., et al., 2009. Apatite (U-Th)/He Thermochronometry Using a Radiation Damage Accumulation and Annealing Model. *Geochimica et Cosmochimica Acta*, 73(8): 2347–2365. <https://doi.org/10.1016/j.gca.2009.01.015>
- Flowers, R. M., Shuster, D. L., Wernicke, B. P., et al., 2007. Radiation Damage Control on Apatite (U-Th)/He Dates from the Grand Canyon Region, Colorado Plateau. *Geology*, 35(5): 447–450. <https://doi.org/10.1130/g23471a.1>
- Flowers, R. M., Wernicke, B. P., Farley, K. A., 2008. Unroofing, Incision, and Uplift History of the Southwestern Colorado Plateau from Apatite (U-Th)/He Thermochronometry. *Geological Society of America Bulletin*, 120(5–6): 571–587. <https://doi.org/10.1130/b26231.1>
- Flowers, R. M., Zeitler, P. K., Danišik, M., et al., 2023a. (U-Th)/He Chronology: Part 1. Data, Uncertainty, and Reporting. *GSA Bulletin*, 135(1–2): 104–136. <https://doi.org/10.1130/b36266.1>
- Foeken, J. P. T., Stuart, F. M., Dobson, K. J., et al., 2006. A Diode Laser System for Heating Minerals for (U-Th)/He Chronometry. *Geochemistry, Geophysics, Geosystems*, 7(4): 1–9. <https://doi.org/10.1029/2005gc001190>
- Gautheron, C., Barbarand, J., Ketcham, R. A., et al., 2013. Chemical Influence on α -Recoil Damage Annealing in Apatite: Implications for (U-Th)/He Dating. *Chemical Geology*, 351: 257–267. <https://doi.org/10.1016/j.chemgeo.2013.05.027>
- Gautheron, C., Tassan-Got, L., Ketcham, R. A., et al., 2012. Accounting for Long Alpha-Particle Stopping Distances in (U-Th-Sm)/He Geochronology: 3D Modeling of Diffusion, Zoning, Implantation, and Abrasion. *Geochimica et Cosmochimica Acta*, 96: 44–56. <https://doi.org/10.1016/j.gca.2012.08.016>
- Gibbons, J. F., 1972. Ion Implantation in Semiconductors: Part II: Damage Production and Annealing. *Proceedings of the IEEE*, 60(9): 1062–1096. <https://doi.org/10.1109/proc.1972.8854>
- Ginster, U., Reiners, P. W., Nasdala, L., et al., 2019. Annealing Kinetics of Radiation Damage in Zircon. *Geochimica et Cosmochimica Acta*, 249: 225–246. <https://doi.org/10.1016/j.gca.2019.01.033>
- Gleadow, A., Harrison, M., Kohn, B., et al., 2015. The Fish Canyon Tuff: A New Look at an Old Low-Temper-

- ature Thermochronology Standard. *Earth and Planetary Science Letters*, 424: 95–108. <https://doi.org/10.1016/j.epsl.2015.05.003>
- Groënlie, A., Harder, V., Roberts, D., 1990. Preliminary Fission - Track Ages of Fluorite Mineralisation along Fracture Zones, Inner Trondheimsfjord, Central Norway. *Norsk Geologisk Tidsskrift*, 70(3): 173–178.
- Guenther, W. R., Reiners, P. W., Ketcham, R. A., et al., 2013. Helium Diffusion in Natural Zircon: Radiation Damage, Anisotropy, and the Interpretation of Zircon (U-Th)/He Thermochronology. *American Journal of Science*, 313(3): 145–198. <https://doi.org/10.2475/03.2013.01>
- Guo, C., Zhang, Z. Y., Wu, L., et al., 2022. Mesozoic-Cenozoic Coupling Process of Tianshan Denudation and Sedimentation in the Northern Margin of the Tarim Basin: Evidence from Low-Temperature Thermochronology (Kuqa River Section, Xinjiang). *Earth Science*, 47(9): 3417–3430 (in Chinese with English abstract).
- Hart, S. R., 1984. He Diffusion in Olivine. *Earth and Planetary Science Letters*, 70(2): 297–302. [https://doi.org/10.1016/0012-821x\(84\)90014-1](https://doi.org/10.1016/0012-821x(84)90014-1)
- Heim, J. A., Vasconcelos, P. M., Shuster, D. L., et al., 2006. Dating Paleochannel Iron Ore by (U - Th)/He Analysis of Supergene Goethite, Hamersley Province, Australia. *Geology*, 34(3): 173–176. <https://doi.org/10.1130/G22003.1>
- Hofmann, F., Treffkorn, J., Farley, K. A., 2020. U-Loss Associated with Laser-Heating of Hematite and Goethite in Vacuum during (U-Th)/He Dating and Prevention Using High O₂ Partial Pressure. *Chemical Geology*, 532: 119350. <https://doi.org/10.1016/j.chemgeo.2019.119350>
- Hourigan, J. K., Reiners, P. W., Brandon, M. T., 2005. U-Th Zonation-Dependent Alpha-Ejection in (U-Th)/He Chronometry. *Geochimica et Cosmochimica Acta*, 69(13): 3349–3365. <https://doi.org/10.1016/j.gca.2005.01.024>
- House, M. A., Farley, K. A., Stockli, D. F., 2000. Helium Chronometry of Apatite and Titanite Using Nd-YAG Laser Heating. *Earth and Planetary Science Letters*, 183(3–4): 365–368. [https://doi.org/10.1016/S0012-821x\(00\)00286-7](https://doi.org/10.1016/S0012-821x(00)00286-7)
- House, M. A., Wernicke, B. P., Farley, K. A., et al., 1997. Cenozoic Thermal Evolution of the Central Sierra Nevada, California, from (U-Th)/He Thermochronometry. *Earth and Planetary Science Letters*, 151(3–4): 167–179. [https://doi.org/10.1016/S0012-821x\(97\)81846-8](https://doi.org/10.1016/S0012-821x(97)81846-8)
- Howie, R. A., Zussman, J., Deer, W. 1992. An Introduction to the Rock-Forming Minerals (Second Edition). Longman Scientific and Technical Press, London.
- Idleman, B. D., Zeitler, P. K., McDannell, K. T., 2018. Characterization of Helium Release from Apatite by Continuous Ramped Heating. *Chemical Geology*, 476: 223–232. <https://doi.org/10.1016/j.chemgeo.2017.11.019>
- Jellinek, A. M., Kerr, R. C., 1999. Mixing and Compositional Stratification Produced by Natural Convection: 2. Applications to the Differentiation of Basaltic and Silicic Magma Chambers and Komatiite Lava Flows. *Journal of Geophysical Research: Solid Earth*, 104(B4): 7203–7218. <https://doi.org/10.1029/1998jb900117>
- Johnson, J. E., Flowers, R. M., Baird, G. B., et al., 2017. “Inverted” Zircon and Apatite (U-Th)/He Dates from the Front Range, Colorado: High-Damage Zircon as a Low - Temperature (<50 °C) Thermochronometer. *Earth and Planetary Science Letters*, 466: 80–90. <https://doi.org/10.1016/j.epsl.2017.03.002>
- Jolivet, M., Dempster, T., Cox, R., 2003. Distribution of U and Th in Apatites: Implications for U-Th/He Thermochronology. *Comptes Rendus-Academie des Sciences. Geoscience*, 335(12): 899–906. <https://doi.org/10.1016/j.crte.2003.08.010>
- Jonckheere, R., 2003. On the Densities of Etchable Fission Tracks in a Mineral and Co-Irradiated External Detector with Reference to Fission - Track Dating of Minerals. *Chemical Geology*, 200(1–2): 41–58. [https://doi.org/10.1016/S0009-2541\(03\)00116-5](https://doi.org/10.1016/S0009-2541(03)00116-5)
- Jourdan, F., Eroglu, E., 2017. ⁴⁰Ar/³⁹Ar and (U-Th)/He Model Age Signatures of Elusive Mercurian and Venusian Meteorites. *Meteoritics & Planetary Science*, 52(5): 884–905. <https://doi.org/10.1111/maps.12838>
- Ketcham, R. A., Gautheron, C., Tassan-Got, L., 2011. Accounting for Long Alpha-Particle Stopping Distances in (U-Th-Sm)/He Geochronology: Refinement of the Baseline Case. *Geochimica et Cosmochimica Acta*, 75(24): 7779–7791. <https://doi.org/10.1016/j.gca.2011.10.011>
- Ketcham, R. A., Guenther, W. R., Reiners, P. W., 2013. Geometric Analysis of Radiation Damage Connectivity in Zircon, and Its Implications for Helium Diffusion. *American Mineralogist*, 98(2–3): 350–360. <https://doi.org/10.2138/am.2013.4249>
- Kraml, M., Pik, R., Rahn, M., et al., 2006. A New Multi-Mineral Age Reference Material for ⁴⁰Ar/³⁹Ar, (U-Th)/He and Fission Track Dating Methods: The Limberg t3 Tuff. *Geostandards and Geoanalytical Research*, 30(2): 73–86. <https://doi.org/10.1111/j.1751-908X.2006.tb00914.x>

- Li, C. P., Zheng, D. W., Zhou, R. J., et al., 2021. Late Oligocene Tectonic Uplift of the East Kunlun Shan: Expansion of the Northeastern Tibetan Plateau. *Geophysical Research Letters*, 48(3): e91281. <https://doi.org/10.1029/2020gl091281>
- Li, X. H., Long, W. G., Li, Q. L., et al., 2010. Penglai Zircon Megacrysts: A Potential New Working Reference Material for Microbeam Determination of Hf-O Isotopes and U-Pb Age. *Geostandards and Geoanalytical Research*, 34(2): 117–134. <https://doi.org/10.1111/j.1751-908x.2010.00036.x>
- Li, Y. J., Zheng, D. W., Wu, Y., et al., 2017. A Potential (U-Th)/He Zircon Reference Material from Penglai Zircon Megacrysts. *Geostandards and Geoanalytical Research*, 41(3): 359–365. <https://doi.org/10.1111/ggr.12168>
- Lin, X., Wu, L., Jolivet, M., et al., 2022. Apatite (U-Th)/He Thermochronology Evidence for Two Cenozoic Denudation Events in Eastern Part of Sulu Orogenic Belt. *Earth Science*, 47(4): 1162–1176 (in Chinese with English abstract).
- Lippolt, H. J., Leitz, M., Wernicke, R. S., et al., 1994. (Uranium+Thorium)/Helium Dating of Apatite: Experience with Samples from Different Geochemical Environments. *Chemical Geology*, 112(1–2): 179–191. [https://doi.org/10.1016/0009-2541\(94\)90113-9](https://doi.org/10.1016/0009-2541(94)90113-9)
- Lippolt, H. J., Weigel, E., 1988. ^4He Diffusion in ^{40}Ar -Retentive Minerals. *Geochimica et Cosmochimica Acta*, 52(6): 1449–1458. [https://doi.org/10.1016/0016-7037\(88\)90215-3](https://doi.org/10.1016/0016-7037(88)90215-3)
- Lippolt, H. J., Wernicke, R. S., Boschmann, W., 1993. ^4He Diffusion in Specular Hematite. *Physics and Chemistry of Minerals*, 20(6): 415–418–418. <https://doi.org/10.1007/BF00203111>
- Liu, J., Zhang, J. Y., McPhillips, D., et al., 2018. Multiple Episodes of Fast Exhumation since Cretaceous in Southeast Tibet, Revealed by Low-Temperature Thermochronology. *Earth and Planetary Science Letters*, 490: 62–76. <https://doi.org/10.1016/j.epsl.2018.03.011>
- McDannell, K. T., Zeitler, P. K., Janes, D. G., et al., 2018a. Screening Apatites for (U-Th)/He Thermochronometry via Continuous Ramped Heating: He Age Components and Implications for Age Dispersion. *Geochimica et Cosmochimica Acta*, 223: 90–106. <https://doi.org/10.1016/j.gca.2017.11.031>
- McDannell, K. T., Zeitler, P. K., Schneider, D. A., 2018b. Instability of the Southern Canadian Shield during the Late Proterozoic. *Earth and Planetary Science Letters*, 490: 100–109. <https://doi.org/10.1016/j.epsl.2018.03.012>
- McDowell, F. W., McIntosh, W. C., Farley, K. A., 2005. A Precise ^{40}Ar - ^{39}Ar Reference Age for the Durango Apatite (U-Th)/He and Fission-Track Dating Standard. *Chemical Geology*, 214(3/4): 249–263. <https://doi.org/10.1016/j.chemgeo.2004.10.002>
- McInnes, B. I. A., Evans, N. J., Fu, F. Q., et al., 2005. Application of Thermochronology to Hydrothermal Ore Deposits. *Reviews in Mineralogy and Geochemistry*, 58(1): 467–498. <https://doi.org/10.2138/rmg.2005.58.18>
- McInnes, B. I. A., Evans, N. J., McDonald, B. J., et al., 2009. Zircon U-Th-Pb-He Bouble Dating of the Merlin Kimberlite Field, Northern Territory, Australia. *Lithos*, 112(S1): 592–599. <https://doi.org/10.1016/j.lith-s.2009.05.006>
- Meesters, A. G. C. A., Dunai, T. J., 2002. Solving the Production-Diffusion Equation for Finite Diffusion Domains of Various Shapes. *Chemical Geology*, 186(1–2): 57–73. [https://doi.org/10.1016/s0009-2541\(01\)00423-5](https://doi.org/10.1016/s0009-2541(01)00423-5)
- Metcalf, J. R., Flowers, R. M. 2013. Initial Development of Baddeleyite (U-Th)/He Thermochronology. The 125th Anniversary Annual Meeting of the Geological Society of America, Denver.
- Min, K., Farley, K. A., Renne, P. R., et al., 2003. Single Grain (U-Th)/He Ages from Phosphates in Acapulco Meteorite and Implications for Thermal History. *Earth and Planetary Science Letters*, 209(3–4): 323–336. [https://doi.org/10.1016/s0012-821x\(03\)00080-3](https://doi.org/10.1016/s0012-821x(03)00080-3)
- Min, K., Reiners, P. W., Nicolescu, S., et al., 2004. Age and Temperature of Shock Metamorphism of Martian Meteorite Los Angeles from (U-Th)/He Thermochronometry. *Geology*, 32(8): 677–680. <https://doi.org/10.1130/g20510.1>
- Min, K., Reiners, P. W., Shuster, D. L., 2013. (U-Th)/He Ages of Phosphates from St. Séverin LL6 Chondrite. *Geochimica et Cosmochimica Acta*, 100: 282–296. <https://doi.org/10.1016/j.gca.2012.09.042>
- Min, K., Reiners, P. W., Wolff, J. A., et al., 2006. (U-Th)/He Dating of Volcanic Phenocrysts with High-U-Th Inclusions, Jemez Volcanic Field, New Mexico. *Chemical Geology*, 227(3–4): 223–235. <https://doi.org/10.1016/j.chemgeo.2005.10.006>
- Monteiro, H. S., Vasconcelos, P. M., Farley, K. A., et al., 2014. (U-Th)/He Geochronology of Goethite and the Origin and Evolution of Cangas. *Geochimica et Cosmochimica Acta*, 131: 267–289. <https://doi.org/10.1016/j.gca.2014.01.036>

- Moreira, M., Blusztajn, J., Curtice, J., et al., 2003. He and Ne Isotopes in Oceanic Crust: Implications for Noble Gas Recycling in the Mantle. *Earth and Planetary Science Letters*, 216(4): 635–643. [https://doi.org/10.1016/s0012-821x\(03\)00554-5](https://doi.org/10.1016/s0012-821x(03)00554-5)
- Moser, A. C., Evans, J. P., Ault, A. K., et al., 2017. (U-Th)/He Thermochronometry Reveals Pleistocene Punctuated Deformation and Synkinematic Hematite Mineralization in the Mecca Hills, Southernmost San Andreas Fault Zone. *Earth and Planetary Science Letters*, 476: 87–99. <https://doi.org/10.1016/j.epsl.2017.07.039>
- Naeser, C. W., Fleischer, R. L., 1975. Age of the Apatite at Cerro de Mercado, Mexico: A Problem for Fission-Track Annealing Corrections. *Geophysical Research Letters*, 2(2): 67–70. <https://doi.org/10.1029/gl002i002p00067>
- Nasdala, L., Reiners, P. W., Garver, J. I., et al., 2004. Incomplete Retention of Radiation Damage in Zircon from Sri Lanka. *American Mineralogist*, 89(1): 219–231. <https://doi.org/10.2138/am-2004-0126>
- Niculescu, S., Reiners, P. W., 2005. (U-Th)/He Dating of Epidote and Andradite Garnet. The 15th Annual V.M. Goldschmidt Conference, Moscow.
- Orme, D. A., Guenther, W. R., Laskowski, A. K., et al., 2016. Long-Term Tectonothermal History of Laramide Basement from Zircon-He Age-eU Correlations. *Earth and Planetary Science Letters*, 453: 119–130. <https://doi.org/10.1016/j.epsl.2016.07.046>
- Pang, J. Z., Yu, J. X., Zheng, D. W., et al., 2019. Neogene Expansion of the Qilian Shan, North Tibet: Implications for the Dynamic Evolution of the Tibetan Plateau. *Tectonics*, 38(3): 1018–1032. <https://doi.org/10.1029/2018tc005258>
- Parrish, R. R., 1990. U-Pb Dating of Monazite and Its Application to Geological Problems. *Canadian Journal of Earth Sciences*, 27(11): 1431–1450. <https://doi.org/10.1139/e90-152>
- Peeters, F., Beyerle, U., Aeschbach-Hertig, W., et al., 2003. Improving Noble Gas Based Paleoclimate Reconstruction and Groundwater Dating Using $^{20}\text{Ne}/^{22}\text{Ne}$ Ratios. *Geochimica et Cosmochimica Acta*, 67(4): 587–600. [https://doi.org/10.1016/s0016-7037\(02\)00969-9](https://doi.org/10.1016/s0016-7037(02)00969-9)
- Peppe, D. J., Reiners, P. W., 2007. Conodont (U-Th)/He Thermochronology: Initial Results, Potential, and Problems. *Earth and Planetary Science Letters*, 258(3–4): 569–580. <https://doi.org/10.1016/j.epsl.2007.04.022>
- Peterman, E. M., Hourigan, J. K., Grove, M., 2014. Experimental and Geologic Evaluation of Monazite (U-Th)/He Thermochronometry: Catnip Sill, Catalina Core Complex, Tucson, AZ. *Earth and Planetary Science Letters*, 403: 48–55. <https://doi.org/10.1016/j.epsl.2014.06.020>
- Petrus, J. A., Kamber, B. S., 2012. VisualAge: A Novel Approach to Laser Ablation ICP-MS U-Pb Geochronology Data Reduction. *Geostandards and Geoanalytical Research*, 36(3): 247–270. <https://doi.org/10.1111/j.1751-908x.2012.00158.x>
- Phillips, D., Kohn, B. P., Gleadow, A. J., et al., 2007. ^4He Implantation in Natural Diamond: Implications for Apatite (U-Th)/He Thermochronometry. AGU Fall Meeting, San Francisco.
- Pi, T., Solé, J., Taran, Y., 2005. (U-Th)/He Dating of Fluorite: Application to the La Azul Fluorspar Deposit in the Taxco Mining District, Mexico. *Mineralium Deposita*, 39(8): 976–982. <https://doi.org/10.1007/s00126-004-0443-y>
- Pickering, J., Matthews, W., Enkelmann, E., et al., 2020. Laser Ablation (U-Th-Sm)/He Dating of Detrital Apatite. *Chemical Geology*, 548: 119683. <https://doi.org/10.1016/j.chemgeo.2020.119683>
- Porcelli, D., Turekian, K. K., 2003. The History of Planetary Degassing as Recorded by Noble Gases. In: Holland, H. D., Turekian, K. K., eds., *Treatise on Geochemistry*. Elsevier, Amsterdam. <https://doi.org/10.1016/b0-08-043751-6/04181-5>
- Powell, J. W., Schneider, D. A., Issler, D. R., 2018. Application of Multi-Kinetic Apatite Fission Track and (U-Th)/He Thermochronology to Source Rock Thermal History: A Case Study from the Mackenzie Plain, NWT, Canada. *Basin Research*, 30(S1): 497–512. <https://doi.org/10.1111/bre.12233>
- Powell, J., Schneider, D., Stockli, D. F., et al., 2016. Zircon (U-Th)/He Thermochronology of Neoproterozoic Strata from the Mackenzie Mountains, Canada: Implications for the Phanerozoic Exhumation and Deformation History of the Northern Canadian Cordillera. *Tectonics*, 35(3): 663–689. <https://doi.org/10.1002/2015tc003989>
- Reiners, P. W., Farley, K. A., 1999. Helium Diffusion and (U-Th)/He Thermochronometry of Titanite. *Geochimica et Cosmochimica Acta*, 63(22): 3845–3859. [https://doi.org/10.1016/s0016-7037\(99\)00170-2](https://doi.org/10.1016/s0016-7037(99)00170-2)
- Reiners, P. W., Farley, K. A., 2001. Influence of Crystal Size on Apatite (U-Th)/He Thermochronology: An Example from the Bighorn Mountains, Wyoming. *Earth and Planetary Science Letters*, 188(3–4): 413–420. [https://doi.org/10.1016/s0012-821x\(01\)00341-7](https://doi.org/10.1016/s0012-821x(01)00341-7)

- Reiners, P. W., Farley, K. A., Hickey, H. J., 2002. He Diffusion and (U-Th)/He Thermochronometry of Zircon: Initial Results from Fish Canyon Tuff and Gold Butte. *Tectonophysics*, 349(1-4): 297-308. [https://doi.org/10.1016/s0040-1951\(02\)00058-6](https://doi.org/10.1016/s0040-1951(02)00058-6)
- Reiners, P. W., Spell, T. L., Nicolescu, S., et al., 2004. Zircon (U-Th)/He Thermochronometry: He Diffusion and Comparisons with $^{40}\text{Ar}/^{39}\text{Ar}$ Dating. *Geochimica et Cosmochimica Acta*, 68(8): 1857-1887. <https://doi.org/10.1016/j.gca.2003.10.021>
- Robinson, K. H., Flowers, R. M., Metcalf, J. R., 2019. Rutile (U-Th)/He Thermochronology: Temperature Sensitivity and Radiation Damage Effects. *Geochemistry, Geophysics, Geosystems*, 20(11): 4737-4755. <https://doi.org/10.1029/2019gc008484>
- Schmitt, A. K., Danišik, M., Aydar, E., et al., 2014. Identifying the Volcanic Eruption Depicted in a Neolithic Painting at Çatalhöyük, Central Anatolia, Turkey. *PLoS One*, 9(1): e84711. <https://doi.org/10.1371/journal.pone.0084711>
- Schmitt, A. K., Martin, A., Stockli, D. F., et al., 2013. (U-Th)/He Zircon and Archaeological Ages for a Late Prehistoric Eruption in the Salton Trough (California, USA). *Geology*, 41(1): 7-10. <https://doi.org/10.1130/g33634.1>
- Schwartz, S., Gautheron, C., Ketcham, R. A., et al., 2020. Unraveling the Exhumation History of High-Pressure Ophiolites Using Magnetite (U-Th-Sm)/He Thermochronometry. *Earth and Planetary Science Letters*, 543: 116359. <https://doi.org/10.1016/j.epsl.2020.116359>
- Seman, S., Stockli, D. F., Smye, A. J., et al., 2014. Garnet (U-Th)/He Thermochronometry and Its Application to Exhumed High-pressure Low-temperature Metamorphic Rocks. 14th International Conference on Thermochronology, Chamonix.
- Shuster, D. L., Farley, K. A., 2009. The Influence of Artificial Radiation Damage and Thermal Annealing on Helium Diffusion Kinetics in Apatite. *Geochimica et Cosmochimica Acta*, 73(1): 183-196. <https://doi.org/10.1016/j.gca.2008.10.013>
- Shuster, D. L., Flowers, R. M., Farley, K. A., 2006. The Influence of Natural Radiation Damage on Helium Diffusion Kinetics in Apatite. *Earth and Planetary Science Letters*, 249(3-4): 148-161. <https://doi.org/10.1016/j.epsl.2006.07.028>
- Spiegel, C., Kohn, B., Belton, D., et al., 2009. Apatite (U-Th-Sm)/He Thermochronology of Rapidly Cooled Samples: The Effect of He Implantation. *Earth and Planetary Science Letters*, 285(1-2): 105-114. <https://doi.org/10.1016/j.epsl.2009.05.045>
- Stanley, J. R., Flowers, R. M., 2016. Dating Kimberlite Emplacement with Zircon and Perovskite (U-Th)/He Geochronology. *Geochemistry, Geophysics, Geosystems*, 17(11): 4517-4533. <https://doi.org/10.1002/2016gc006519>
- Stockli, D. F., Farley, K. A., 2004. Empirical Constraints on the Titanite (U-Th)/He Partial Retention Zone from the KTB Drill Hole. *Chemical Geology*, 207(3-4): 223-236. <https://doi.org/10.1016/j.chemgeo.2004.03.002>
- Stockli, D. F., Wolfe, M. R., Blackburn, T. J., et al., 2007. He Diffusion and (U-Th)/He Thermochronometry of Rutile. AGU Fall Meeting, San Francisco.
- Sun, J. B., Chen, W., Yu, S., et al., 2017. Study on Zircon (U-Th)/He Dating Technique. *Acta Petrologica Sinica*, 33(6): 1947-1956 (in Chinese with English abstract).
- Tagami, T., Farley, K. A., Stockli, D. F., 2003. (U-Th)/He Geochronology of Single Zircon Grains of Known Tertiary Eruption Age. *Earth and Planetary Science Letters*, 207(1-4): 57-67. [https://doi.org/10.1016/s0012-821x\(02\)01144-5](https://doi.org/10.1016/s0012-821x(02)01144-5)
- Tao, N., Li, Z. X., Danišik, M., et al., 2019. Post-250 Ma Thermal Evolution of the Central Cathaysia Block (SE China) in Response to Flat-Slab Subduction at the Proto-Western Pacific Margin. *Gondwana Research*, 75: 1-15. <https://doi.org/10.1016/j.jgr.2019.03.019>
- Tian, Y. T., Qiu, N. S., Kohn, B. P., et al., 2012. Detrital Zircon (U-Th)/He Thermochronometry of the Mesozoic Daba Shan Foreland Basin, Central China: Evidence for Timing of Post-Orogenic Denudation. *Tectonophysics*, 570-571: 65-77. <https://doi.org/10.1016/j.tecto.2012.08.010>
- Tian, Y. T., Vermeesch, P., Danišik, M., et al., 2017. LGC-1: A Zircon Reference Material for In-Situ (U-Th)/He Dating. *Chemical Geology*, 454: 80-92. <https://doi.org/10.1016/j.chemgeo.2017.02.026>
- Tripathy-Lang, A., Hodges, K. V., Monteleone, B. D., et al., 2013. Laser (U-Th)/He Thermochronology of Detrital Zircons as a Tool for Studying Surface Processes in Modern Catchments. *Journal of Geophysical Research: Earth Surface*, 118(3): 1333-1341. <https://doi.org/10.1002/jgrf.20091>
- Trull, T. W., Kurz, M. D., 1993. Experimental Measurements of ^3He and ^4He Mobility in Olivine and Clinopyroxene at Magmatic Temperatures. *Geochimica et Cosmochimica Acta*, 57(6): 1313-1324. <https://doi.org/10.1016/j.gca.2003.10.021>

- 10.1016/0016-7037(93)90068-8
- Tyrrell, J. P., Bidgoli, T. S., Möller, A., et al., 2016. Challenges Associated with the Conodont (U-Th)/He Method: A Case Study from the Mormon Mountains, Tule Spring Hills, and Beaver Dam Mountains, South-eastern Nevada and Southwestern Utah. GSA Annual Meeting, Denver. <https://doi.org/10.1130/abs/2016am-286505>
- van Soest, M. C., Hodges, K. V., Wartho, J. A., et al., 2011. (U-Th)/He Dating of Terrestrial Impact Structures: The Manicouagan Example. *Geochemistry, Geophysics, Geosystems*, 12(5): Q0AA16. <https://doi.org/10.1029/2010gc003465>
- van Soest, M. C., Monteleone, B. D., Boyce, J. W., et al., 2008. Advances in Laser Microprobe (U-Th)/He Geochronology. AGU Fall Meeting, San Francisco.
- Vasconcelos, P. M., Heim, J. A., Farley, K. A., et al., 2013. $^{40}\text{Ar}/^{39}\text{Ar}$ and (U-Th)/He- $^4\text{He}/^3\text{He}$ Geochronology of Landscape Evolution and Channel Iron Deposit Genesis at Lynn Peak, Western Australia. *Geochimica et Cosmochimica Acta*, 117: 283–312. <https://doi.org/10.1016/j.gca.2013.03.037>
- Vermeesch, P., Seward, D., Latkoczy, C., et al., 2007. A-Emitting Mineral Inclusions in Apatite, Their Effect on (U-Th)/He Ages, and How to Reduce It. *Geochimica et Cosmochimica Acta*, 71(7): 1737–1746. <https://doi.org/10.1016/j.gca.2006.09.020>
- Wang, F., Feng, H. L., Shi, W. B., et al., 2016. Relief History and Denudation Evolution of the Northern Tibet Margin: Constraints from $^{40}\text{Ar}/^{39}\text{Ar}$ and (U-Th)/He Dating and Implications for Far-Field Effect of Rising Plateau. *Tectonophysics*, 675: 196–208. <https://doi.org/10.1016/j.tecto.2016.03.001>
- Wang, W. T., Zheng, D. W., Li, C. P., et al., 2020. Cenozoic Exhumation of the Qilian Shan in the Northeastern Tibetan Plateau: Evidence from Low-Temperature Thermochronology. *Tectonics*, 39(4): e2019TC005705. <https://doi.org/10.1029/2019tc005705>
- Wang, Y. Z., Li, C. P., Hao, Y. Q., et al., 2022. Multi-Stage Growth in the North Margin of the Qinling Orogen, Central China, Revealed by both Low-Temperature Thermochronology and River Profile Inversion. *Tectonics*, 41(4): e2021TC007029. <https://doi.org/10.1029/2021TC007029>
- Wang, Y., Zheng, D. W., Li, Y. J., et al., 2019. (U-Th)/He Dating of International Standard Fish Canyon Tuff Zircon. *Seismology and Geology*, 41(5): 1302–1315 (in Chinese with English abstract).
- Wang, Y., Zheng, D. W., Wu, Y., et al., 2017. Measurement Procedure of Single-Grain Apatite (U-Th)/He Dating and Its Validation by Durango Apatite Standard. *Seismology and Geology*, 39(6): 1143–1157 (in Chinese with English abstract).
- Willett, C. D., Fox, M., Shuster, D. L., 2017. A Helium-Based Model for the Effects of Radiation Damage Annealing on Helium Diffusion Kinetics in Apatite. *Earth and Planetary Science Letters*, 477: 195–204. <https://doi.org/10.1016/j.epsl.2017.07.047>
- Wolf, R. A., Farley, K. A., Kass, D. M., 1998. Modeling of the Temperature Sensitivity of the Apatite (U-Th)/He Thermochronometer. *Chemical Geology*, 148 (1–2): 105–114. [https://doi.org/10.1016/s0009-2541\(98\)00024-2](https://doi.org/10.1016/s0009-2541(98)00024-2)
- Wolf, R. A., Farley, K. A., Silver, L. T., 1996. Helium Diffusion and Low-Temperature Thermochronometry of Apatite. *Geochimica et Cosmochimica Acta*, 60(21): 4231–4240. [https://doi.org/10.1016/s0016-7037\(96\)00192-5](https://doi.org/10.1016/s0016-7037(96)00192-5)
- Wolff, R., Dunkl, I., Kempe, U., et al., 2016. Variable Helium Diffusion Characteristics in Fluorite. *Geochimica et Cosmochimica Acta*, 188: 21–34. <https://doi.org/10.1016/j.gca.2016.05.029>
- Wu, L. Q., Jiao, Y. Q., Wang, G. R., et al., 2022. Response of Uranium Mineralization in Kuqa Depression Driven by Basin-Mountain Coupling Mechanism. *Earth Science*, 47(9): 3174–3191 (in Chinese with English abstract).
- Wu, L., Shi, G. H., Danišik, M., et al., 2019. MK-1 Apatite: A New Potential Reference Material for (U-Th)/He Dating. *Geostandards and Geoanalytical Research*, 43 (2): 301–315. <https://doi.org/10.1111/ggr.12258>
- Yang, J., Zheng, D. W., Chen, W., et al., 2014. Apatite $^4\text{He}/^3\text{He}$ Thermochronometry: A New Method of Low Temperature Thermochronometry. *Seismology and Geology*, 36(4): 1009–1019 (in Chinese with English abstract).
- Yang, L., Yuan, W. M., Wang, K., 2018. Research Advances of Thermochronology in Mineral Deposits. *Earth Science*, 43(6): 1887–1902 (in Chinese with English abstract).
- Yang, L., Yuan, W. M., Zhu, C. B., et al., 2021. Mesozoic Uplift Exhumation History of East Kunlun. *Acta Petrologica Sinica*, 37(12): 3781–3796 (in Chinese with English abstract).
- Yu, J. X., Zheng, D. W., Pang, J. Z., et al., 2019. Miocene Range Growth along the Altyn Tagh Fault: Insights from Apatite Fission Track and (U-Th)/He Ther-

- mochronometry in the Western Danghenan Shan, China. *Journal of Geophysical Research: Solid Earth*, 124(8): 9433–9453. <https://doi.org/10.1029/2019jb017570>
- Yu, J. X., Zheng, D. W., Zhang, H. P., et al., 2022. Initial Cenozoic Exhumation of the Northern Chinese Tian Shan Deduced from Apatite (U-Th)/He Thermochronological Data. *Lithosphere*, 2022(1): 8099539. <https://doi.org/10.2113/2022/8099539>
- Yu, S., Chen, W., Sun, J. B., 2019. Diffusion of Helium in FCT Zircon. *Science in China (Series D)*, 49(4): 656–670 (in Chinese with English abstract).
- Yu, S., Sun, J. B., Evans, N. J., et al., 2020. Further Evaluation of Penglai Zircon Megacrysts as a Reference Material for (U-Th)/He Dating. *Geostandards and Geoanalytical Research*, 44(4): 763–783. <https://doi.org/10.1111/ggr.12331>
- Yu, S., Tian, Y. T., 2023. Helium Diffusion and (U-Th)/He Thermochronology on Fish Canyon Tuff Titanite. *Acta Geologica Sinica*, 97(1): 278–290 (in Chinese with English abstract).
- Yu, Y., Xu, X. S., Chen, X. M., 2010. Genesis of Zircon Megacrysts in Cenozoic Alkali Basalts and the Heterogeneity of Subcontinental Lithospheric Mantle, Eastern China. *Mineralogy and Petrology*, 100(1–2): 75–94. <https://doi.org/10.1007/s00710-010-0120-z>
- Yuan, W. M., 2016. Thermochronological Method of Revealing Conservation and Changes of Mineral Deposits. *Acta Petrologica Sinica*, 32(8): 2571–2578 (in Chinese with English abstract).
- Zeitler, P. K., Herczeg, A. L., McDougall, I., et al., 1987. U-Th-He Dating of Apatite: A Potential Thermochronometer. *Geochimica et Cosmochimica Acta*, 51(10): 2865–2868. [https://doi.org/10.1016/0016-7037\(87\)90164-5](https://doi.org/10.1016/0016-7037(87)90164-5)
- Zhang, B., Chen, W., Liu, J. Q., et al., 2020. Thermochronological Insights into the Intracontinental Orogeny of the Chinese Western Tianshan Orogen. *Journal of Asian Earth Sciences*, 194: 103927. <https://doi.org/10.1016/j.jseaes.2019.103927>
- Zheng, D. W., Wu, Y., Pang, J. Z., et al., 2016. Fundamentals, Dating and Application of U-Th/He Thermochronology. *Quaternary Sciences*, 36(5): 1027–1036 (in Chinese with English abstract).
- Zheng, D. W., Zhang, P. Z., Wan, J. L., et al., 2006. Rapid Exhumation at ~8 Ma on the Liupan Shan Thrust Fault from Apatite Fission-Track Thermochronology: Implications for Growth of the Northeastern Tibetan Plateau Margin. *Earth and Planetary Science Letters*, 248(1–2): 198–208. <https://doi.org/10.1016/j.epsl.2006.05.023>

中文参考文献

- 蔡长娥, 陈鸿, 尚文亮, 等, 2020a. 牙形石(U-Th)/He热定年技术的研究进展. *地球科学进展*, 35(9): 924–932.
- 蔡长娥, 邱楠生, 李慧莉, 等, 2020b. 自然演化碎屑锆石(U-Th)/He封闭温度的研究. *中国科学(D辑)*, 50(1): 66–78.
- 冯乾乾, 邱楠生, 常健, 等, 2018. 房山岩体构造-热演化: 来自(U-Th)/He年龄的约束. *地球科学*, 43(6): 1972–1982.
- 郭超, 张志勇, 吴林, 等, 2022. 中生代天山剥蚀与塔里木盆地北缘沉积耦合过程: 新疆库车河剖面的低温热年代学证据. *地球科学*, 47(9): 3417–3430.
- 林旭, 吴林, Jolivet, M., 等, 2022. 苏鲁造山带东段新生代两阶段剥露事件的磷灰石(U-Th)/He热年代学证据. *地球科学*, 47(4): 1162–1176.
- 孙敬博, 陈文, 喻顺, 等, 2017. 锆石(U-Th)/He定年技术研究. *岩石学报*, 33(6): 1947–1956.
- 王英, 郑德文, 李又娟, 等, 2019. 国际标样Fish Canyon Tuff锆石的(U-Th)/He年龄测定. *地震地质*, 41(5): 1302–1315.
- 王英, 郑德文, 武颖, 等, 2017. 磷灰石单颗粒(U-Th)/He热定年实验流程的建立及验证. *地震地质*, 39(6): 1143–1157.
- 吴立群, 焦养泉, 王国荣, 等, 2022. 盆山耦合机制驱动下的库车坳陷铀成矿作用响应. *地球科学*, 47(9): 3174–3191.
- 杨静, 郑德文, 陈文, 等, 2014. 磷灰石⁴He/³He热年代学: 一种低温热年代学研究的新技术. *地震地质*, 36(4): 1009–1019.
- 杨莉, 袁万明, 王珂, 2018. 热年代学方法、技术手段及其在矿床地质中的研究进展. *地球科学*, 43(6): 1887–1902.
- 杨莉, 袁万明, 朱传宝, 等, 2021. 东昆仑中生代隆升剥露历史. *岩石学报*, 37(12): 3781–3796.
- 喻顺, 陈文, 孙敬博, 等, 2019. 锆石He扩散行为: FCT锆石扩散实验的制约. *中国科学(D辑)*, 49(4): 656–670.
- 喻顺, 田云涛, 2023. Fish Canyon Tuff 锆石He扩散及(U-Th)/He年代学研究. *地质学报*, 97(1): 278–290.
- 袁万明, 2016. 矿床保存变化研究的热年代学技术方法. *岩石学报*, 32(8): 2571–2578.
- 郑德文, 武颖, 庞建章, 等, 2016. U-Th/He热年代学原理、测试及应用. *第四纪研究*, 36(5): 1027–1036.